NASA Contractor Report 191056

Phase Linearity of the 914H Coupled-Cavity Traveling Wave Tube

Frank E. Kavanagh
Analex Corporation
Brook Park, Ohio

January 1994

Prepared for
Lewis Research Center
Under Contract NAS3–25776

National Aeronautics and Space Administration

PHASE LINEARITY OF THE 914H COUPLED-CAVITY TRAVELING WAVE TUBE

Frank Kavanagh
Analex Corporation
3001 Aerospace Parkway
Brook Park, Ohio 44142

SUMMARY

Tests of phase deviation from linearity were made on two 914H coupled-cavity traveling wave tubes (TWT). One tube had a voltage standing wave ratio (VSWR) of 2.4 and the other, 1.4. The data showed that phase deviation is primarily a function of the amplitude and shape of the output VSWR. It was predicted that the low-VSWR tube would give better system performance than the tube with a high VSWR. This prediction was confirmed by the Advanced Communications Technology Satellite (ACTS) system tests performed at the NASA Lewis Research Center. A possible improvement in the construction and stability of coupled-cavity TWT's is discussed.

INTRODUCTION

To insure minimum phase distortion, a minimum change of gain versus frequency is a highly desirable characteristic of amplifiers to be used in communication systems. The physical reasons for deviation from phase linearity are primarily related to mismatches both internal and external. Some are caused by changes in the circuit due to fabrication tolerances or by the motion of the circuit from thermal cycling. Others result from variations in the concentration or location of the lossy material used for the internal attenuator and from reflections at the junction of the slow-wave circuit and the radiofrequency output line. The presence of the electron beam in a TWT introduces additional reflections that are not present in the cold tube. These reflections in coupled-cavity tubes can exceed the cold reflections that can occur and can be an order of magnitude larger than those in helix TWT's (ref. 1).

BACKGROUND

The source of gain ripple is the feedback mechanism caused by the reflection of the forward waves in the backward direction and by the reflection of the backward waves in the forward direction. All of these mismatches interact and are enhanced by the gain of the TWT. In coupled-cavity tubes, the problem is the same magnitude as that when one must match a large number of series lossless microwave components having an output return loss (VSWR) of 1.10 or better and maintain this match over large temperature variations (ref. 2). In examining the gain ripple of a TWT, we find that the phase peaks (and valleys) occur at the point where the slope of the gain ripple is maximum. The quadrature relationship between amplitude and phase ripple can be explained by considering the gain ripple as a frequency-sensitive feedback vector added to the normal gain vector, as shown in figure 1. If we consider the gain vector to be rotating at the end of the nominal gain vector as a result of the forward and backward wave interactions, then the phase deviation is the angle between the resultant vector and the average phase vector.

With reference to figure 1, the magnitude of the phase deviation can be related to that of the power gain ripple as follows:

$$\frac{P_{max}}{P_{min}} = \left(\frac{1 + V_{RF}}{1 - V_{RF}}\right)^2$$

where

$$\frac{P_{max}}{P_{min}} = \frac{\text{maximum power in rippled response}}{\text{power at minimum next to the power maximum}}$$

V_{RF} = radiofrequency voltage halfway between maximum and minimum peaks in power

These equations show that a ±1-dB gain ripple results in a ±7° phase ripple.

Although gain compression at saturation and beam deceleration in the output section complicate the phase ripple relationship, the above model gives reasonable agreement. As a TWT is driven over its frequency range from linear low-level operation toward saturation, those frequencies at which the maxima of gain ripple occur are driven further into saturation and incur a greater compression than those frequencies at which a minimum exists. Therefore, an overall flattening of the gain ripple curve occurs at saturation.

When considering phase distortion (other than reflections) in TWT's, Beam and Blattner (ref. 3) derived a relationship which predicts phase deviation to the first order. They found that the phase output used in large-signal operation deviates at saturation from that used in small-signal operation by

$$\Delta\phi = K \times \frac{P_0}{P_{dc}} \times \frac{1}{C}$$

where

$\Delta\phi$ = phase ripple, $\simeq \frac{\Delta V_{RF}}{V_{RF}}$

ΔV_{RF} = radiofrequency voltage ripple amplitude (radians) for small variations

K = constant that depends upon individual tube design

P_0/P_{dc} = electronic efficiency

C = Pierce's gain parameter (proportional to cube root of current)

This equation implies that the phase deviation can be reduced by maximizing the gain parameter C and minimizing the electronic efficiency P_0/P_{dc}, a rather harsh measure in most cases. An explanation is that in the saturation region the electron beam transfers energy to the circuit and in so doing slows down. The phase relationship between the beam and the circuit wave differs from that in the small-signal region, and the difference is integrated over the saturated region. In order to correct this, most tubes have a velocity taper towards the output; that is, the circuit is modified so that the phase velocity of the circuit wave also decreases and therefore stays in synchronism with the bunches in the beam, which improves phase performance. This is especially true with the new dynamic velocity tapers.

Figure 2 from Chaffee (ref. 4) shows a coupled-cavity computer program relating the tube efficiency η, the gain per wavelength G_λ, and the ratio η/G_λ with the synchronism parameter b which is a measure of the velocity difference between the electron beam and the slow-wave structure. Synchronism occurs at b equals 0;

a positive b means that the beam travels faster than the circuit, and a negative b slower than the circuit. In the case considered, the space charge factor QC is 0.25 and C is 0.1. The ratio of efficiency to gain per wavelength was shown earlier to be proportional to the phase deviation. Consider the overvoltage case where b is greater than b_0, the value of b for maximum gain (in this case b = 1). The efficiency is high and the gain per wavelength is reduced from its maximum value; thus, the distortion is high. The greater the overvoltage the higher the distortion. As the cathode voltage is reduced, the efficiency falls off whereas the gain per wavelength first increases to its maximum and then decreases slowly. The distortion then decreases until the gain falls off faster than the efficiency, at which point the minimum distortion has been reached.

An AM-to-PM conversion (fig. 3) is defined as the rate of change of the output phase with respect to an amplitude change of RF input power. In the small-signal region both the phase output deviation and the AM-PM conversion are small. As the tube is driven into large-signal operation, the phase deviation and the AM-PM conversion increase. Note that the AM-PM actually reaches a peak before saturation. Chaffee's studies showed that the best circuit for AM-PM conversion is one in which the circuit velocity is always higher than the beam velocity (i.e., the circuit is undervoltaged) and that the undervoltage has a lesser effect at high frequencies than at low frequencies. Experiments have shown that in coupled-cavity tubes for a given voltage the best results for AM-PM conversion are obtained at the low-frequency end of the hot bandwidth.

The loss parameter d is a measure of the circuit loss and has a large effect on the AM-PM conversion. The dependence of AM-PM on circuit loss was treated by both Ober (ref. 5) and Nishihara (ref. 6). Ober contends that the circuit loss is detrimental because it limits the degree of saturation, the beam modulation, and the negative phase generation. By moving the attenuator section toward the input of the tube, Ober demonstrated significant AM-PM improvement. Nishihara made similar measurements and concluded that the "phase deviation increases exponentially...when the length of the output section decreases or when the attenuator is shifted towards the output side...; it is found that the effect of the attenuator is negligible when the small-signal gain of the output section is more than about 25 dB."

The space change factor QC can affect phase distortion. If QC is low, the circuit forces are much stronger than the space charge forces, and the nonlinear effects such as phase distortion are minimized.

EXPERIMENT

The tube available for the phase distortion measurements was the 914H, manufactured by Hughes Aircraft Co. This tube was not designed specifically for low-distortion operation but is in the frequency range (30 GHz) and has the power output (150 W) of interest for the Advanced Communications Technology Satellite (ACTS) at the NASA Lewis Research Center.

The phase linearity of two tubes was measured over a frequency range of 29 to 32 GHz at a nominal 16.0 kV and 65 mA. The major difference between them is that tube 1 has an anode grounded internally whereas tube 2 has an anode that operates at 100 V with respect to ground. Thus, we could vary the current on 2 but not on 1. Second, cold tests (figs. 4 and 5) determined that the output VSWR of tube 2 was far superior to that of tube 1, an indication that the small-signal gain variations of tube 1 would be much higher than those of tube 2, as was proven to be the case. The instrument used for the measurements was the 8409 network analyzer modified for this project.

During measurements at the various power levels, the RF input to the tube was held constant over the frequency range to within ±0.1 dB at each level. Saturation is not necessarily a well-defined point but occurs over a range of power inputs as shown in figures 6 to 8. There is therefore some ambiguity in defining this point several decibels above and below it. However, once the drive level that determined saturation was settled

upon, it was strictly adhered to in all measurements. During the initial setup, a voltage and frequency were picked so that the tube could be driven to saturation with the least amount of ripple over the range of interest. For example, figures 6 to 8 present the transfer characteristics of tube 2 at 16.0, 16.25, and 16.5 kV, respectively, at different frequencies overlapping the band of interest. If one were to use a different frequency range, a different reference frequency would probably be necessary. At the three operating voltages, 29.75 GHz (the center of the frequency range of interest) was used for the reference saturation frequency, and before every set of measurements the tube was saturated at 29.75 GHz. These figures also demonstrate the variation in gain with voltage and the overall minimization of that variation as one goes to lower voltages. The lower the operating voltage the smaller the gain variation at and well into saturation, albeit at the loss of overall gain. However, this translates into a lower phase distortion as discussed earlier in this section. Figures 9 and 10 show that the gain flatness varies as the tubes are driven from the small-signal region into the saturated region. The cathode voltage in this case was 16.0 kV. Figures 11 and 12 show that the saturated gain of both tubes varies with frequency and that the bandpass changes with voltage. The same gain patterns at saturation from tube to tube are shown at the various voltage levels in figures 9 to 12. The indication is that the gain fluctuations at saturation originate from a common source (the output coupling and circuit) which appears after the initial interaction and severing of the beam and circuit. Figure 9 supports this contention by showing the large variation of gain in tube 1 in the linear region. These gain fluctuations due to circuit irregularities are not compressed in the linear region.

Extensive data were taken at 16.0, 16.25, and 16.5 kV and, in the case of tube 2, at different current levels. Areas of investigation were gain, gain variation, phase linearity and its correlation with the VSWR, voltage change, operating point in the band, and use in the ACTS system. The tubes were operated in 2-dB steps from -20 below saturation to 3 dB above saturation where possible. In some cases the available gain of the tube did not always allow operation above +1.5 dB. The appendix (figs. 23 to 51) presents the curves of the gain variation and phase deviation from linearity for both tubes over the range of 28 to 32 GHz and over the smaller range of interest to ACTS, 29.5 to 30 GHz. The data are for voltages of 16.0, 16.25, and 16.5 kV. The curves show that the phase deviation from linearity in both tubes changed very little if at all from -10 to -3 dB below saturation where the gain ripple starts to become depressed. Indeed, in both tubes the phase deviation does not change substantially until well into saturation. If one looks at the output-return-loss (VSWR) curves of the tubes over their operating range and compares them with the curves of phase deviation from linearity, one finds that they have the same number of maxima and minima. Figures 13 and 14 also show that the phase deviations from linearity occur where the slopes of the gain curves are maximum. There is a correlation between the amplitude of the gain ripple and the maxima of the phase distortion curves. The deviations are worse in the linear region but become much less severe in the saturation region because of the clipping action of the tubes. This is most notable in tubes that have bad mismatches at the output (i.e., a high VSWR as in tube 1 compared with tube 2). It should be noted that the phase distortion in the relatively well matched tube 2 becomes "straightened out" or more constant with frequency as it is driven into saturation and beyond.

Figure 15 shows the importance of operating voltage in determining the phase deviations from linearity across the frequency range, even at saturation. These curves, along with those of figures 6 to 8, demonstrate that one may decrease phase deviation from linearity by sacrificing power and gain. However, the power and gain fall off precipitously below 16 kV. Figure 16 demonstrates that in the linear region there is no change in phase deviation with linearity from one operating level to another.

The output VSWR therefore becomes the dominating factor in determining the useability of tubes in phase-modulated systems and the amount of gain ripple-phase linearity tolerated by a system. In the case of the 914H TWT's, tests were conducted to measure the bit error rate (BER) when the RF input power level was changed (ref. 7). These results are summarized in table I. The ACTS 220-Mbps data rate, using serial-minimum-shift-keying (SMSK) modulation, required a bandwidth of at least 1.5 times the data rate for an acceptable transmission path. Therefore, RF testing placed primary emphasis on the 330-MHz-wide band surrounding the 29.75-GHz center frequency.

The power limitations in the frequency conversion system used in the BER tests permitted testing only at the 75-mW drive level and below (see figs. 9 and 10). The reduced RF drive resulted in an increase in gain variation over the 330-MHz-wide passband but still provided relatively flat gain responses to perform BER testing. The gain variations ranged from 2.5 dB at the 100-mW drive level to as much as 7.0 dB at the 1-mW drive (tube 1).

The BER curves obtained from tube 1 tests are shown in figure 17. The disruptive effects of the increasing gain ripple are still apparent as the BER curves move to the right with decreasing drive level. With the tube operating at the 75-mW RF drive level, no perceptible degradation was observed (note that the 75-mW curve overlaps the baseline system curve), which indicates that the tube has successfully amplified the SMSK signal (without appreciable distortion) in the absence of added uplink noise. The reduction of the input drive from 75 to 25 mW produced a degradation of 2.1 dB in E_b/N_0 at a BER of 5×10^{-7}. Small-signal gain fluctuations in the amplifier passband now become apparent. For a drive level of 1 mW, an E_b/N_0 requirement of 15.3 dB was needed to obtain a BER of 5×10^{-7}. In this case, the 18.75-dB overall reduction in input RF drive level resulted in an approximately 3.7-dB higher E_b/N_0 being required to obtain the same bit error rate.

A second TWT was tested to provide data for a comparison of the two tubes. Tube 2, fabricated second in the 914H series, has a much flatter frequency response over the passband of interest. The gain variation suggests that the BER performance of tube 2 would be significantly better than that of tube 1. This suggestion was later confirmed by the data (fig. 18). For each of the drive levels tested, the bit-error-rate curve falls essentially on top of the baseline system curve. With only a 0.25-dB variation in E_b/N_0, these test results approach the accuracy limits of the BER measurement system. Repeated samples of baseline BER data acquired during the calibration yielded a repeatability of ±0.2 dB. As a result, the BER performance of the tube cannot be distinguished from that of the baseline system and therefore can be said to impose little or no signal degradation. Table I summarizes the bit-error-rate performance.

TABLE I.—SUMMARY OF BIT-ERROR-RATE PERFORMANCE

Total RF input drive level, mW	Ratio of bit energy to noise power density,[a] E_b/N_0, dB	
	Tube 1	Tube 2
75	11.7	11.7
50	12.1	11.8
25	13.8	11.5
1	15.3	11.5

[a]Bit error rate, 5×10^{-7}.

One characteristic common to both tubes is a positive gain slope over the 330-MHz passband. This slope increased with the reduction in RF drive level. This effect, somewhat hidden in tube 1, is clearly exhibited in tube 2. In both tubes the gain slope had a minimal effect on BER. Large peak-to-peak gain ripple, most noticeable at small-signal drive levels, was obvious in the frequency response of tube 1. These large, cyclic variations tend to degrade the tube's ability to maintain a BER of 5×10^{-7}. Tube 2, however, did not have this large gain ripple. In general, the test results indicated that a gain ripple introduced by a maximum periodic VSWR of 1.4 did not degrade the signal whereas a VSWR of 2.3 did degrade the signal in the linear region.

Because SMSK demodulation relies on the phase angle of the received signal, it is critical that the TWT not severely distort the signal waveform. If distortion occurs, the demodulator is unable to identify the signal states and a bit error is potentially recorded. A study of the distortion tests conducted on the individual tubes indicated that for the ACTS system, tube 1 would certainly distort the waveform in the small-signal region but tube 2 should not.

Since phase distortion is primarily a function of gain ripple, which is a function of VSWR, it behooves one to build a tube that has a low VSWR, is physically and thermally rugged, and is easily constructed. Such a tube is very expensive ($100 000) and shrinkage is a major problem. Of the two areas of concern, the first is the construction of the tube when there are as many as three serial brazes at temperatures of 900 °C and above. During these brazes, tube cavities and input/output transformers may become distorted. The second concern is that the signal power is highest over the last 10 percent of the tube structure, which leads to higher space change forces spreading the beam and hence higher interception and higher losses in the circuit.

Changes in frequency due to the thermal expansion of the circuit were apparent while the tube was tested. A simple, completely enclosed, 30-GHz re-entrant cavity design is presented in figure 19 along with the sensitivity of the cavity frequency to dimensional changes. When working at saturation or beyond and then switching to allow level of operation, it takes some minutes for the tube to stabilize thermally (i.e., frequency power and gain). Therefore, it was best to run the lower power levels first, moving gradually toward saturation.

The circuit used in the 914H TWT consists of a stack of approximately 100 cavities, such as the Hughes type shown in figure 20(a). This structure, a copper disk with a ferrule on each side, is supported by brazing at its periphery to two copper annular rings. A hundred or more cavities are brazed together. As mentioned, any distortion of a cavity or input-to-output coupler during brazes can affect the VSWR. One way to minimize this problem is to eliminate the ferrules because the gap between ferrules has the greatest influence on frequency change. This simple and straightforward approach has severe drawbacks. First, the electronic efficiency of the circuit drops from 17 to 5 percent and the operating voltage increases by 33 percent; second, the current increases by a factor of 3. It was thought that a different cavity design, specifically a single re-entrant cavity strengthened to be more massive, would have better thermal and construction properties.

Figure 20 shows crossections of the Hughes Cavity (A) and three of the cavities that were designed and tested (B,C,D). For cold tests, the cavities were fabricated at x-band. Cavity B is a straightforward single re-entrant cavity; the design of C improves the conduction of the center of the cavity where the interception is most severe and at the same time increases the thermal capacitance at the edges; and D is the most rugged design in all respects. Figure 21 shows the Pierce impedance K_p curves for all four designs. Both the Hughes (A) and the rugged D design are very close in impedance ($\beta L/\pi = 1.4$): A is 9 ohms and D is 8 ohms. Cavity C has an impedance of 16 ohms, and the simple re-entrant cavity B 12 ohms.

It must be remembered that these cavities are not brazed to an annular ring but are simply stacked one upon the other. In addition, that only one ferrule is needed (and designs C and D are thermally rugged) results in a much more stable construction.

These cavities were designed to operate at the same voltage and current as the 914H. The bandwidth of circuits made from these cavities is shown in figure 22. The substitution of cavity type D would give the same power output as the 914H and increase the bandwidth by 2 percent. The substitution of cavity type C would reduce the bandwidth from 35 to 30 percent but would increase the electronic efficiency by 25 percent. Cavity B would give 2 percent less in bandwidth but would increase the efficiency by 12 percent. With reference to figure 20, it seems probable that instead of machining the cavity elements and brazing them together as in the construction of the 914H, the single re-entrant cavities could be cheaply vapor deposited on a multielement mold from which they could be removed and lapped to their exact height. This procedure would be much less expensive than machining, in addition to allowing a more simple and more rugged fabricating process without compromising the electrical performance of the tube. The results of this study revealed that cavity type D would be the best design for use in traveling-wave-tube circuits.

CONCLUDING REMARKS

Phase linearity measurements were made on the 914H coupled-cavity traveling wave tube. The phase deviation from linearity was shown to be primarily a function of the output voltage standing wave ratio (VSWR) as determined by both tube and system measurements. These measurements revealed that even tubes with a high phase deviation from linearity in the small-signal region may be useful in systems if the tubes are run at saturation. This finding is attributed to the smoothing of the gain variations by the tube at saturation, which results in a decrease in phase nonlinearities. The VSWR can be a function not only of design but of fabrication and operation temperature. A study was made to determine the most rugged design for a tube of this type, the result being a new cusp-shaped single re-entrant cavity.

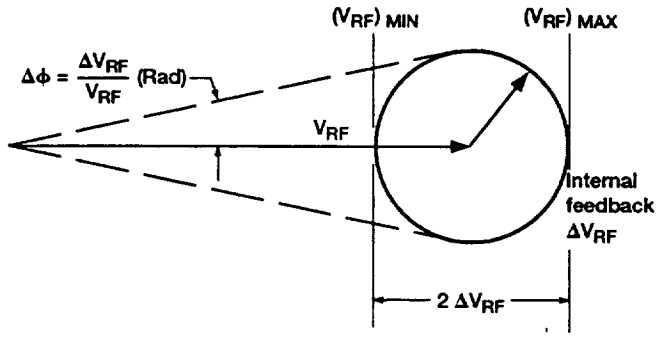

Figure 1.—Gain-phase relationship.

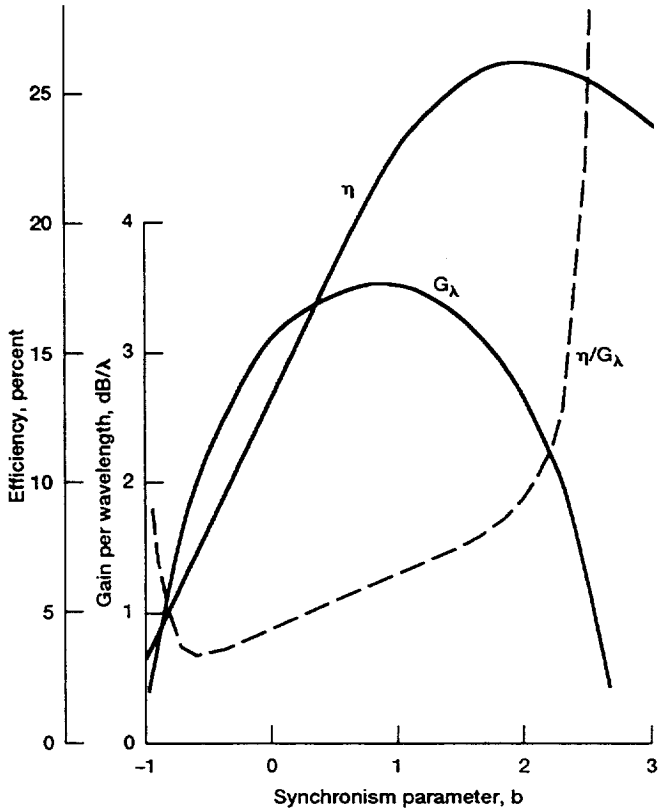

Figure 2.—Small-signal gain and efficiency versus synchronism parameter. Space change factor, 0.25; Pierce gain parameter, 0.1.

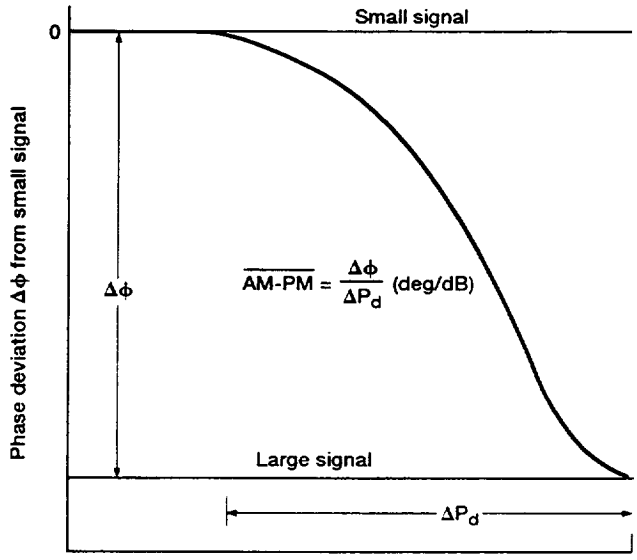

(a) Phase deviation.

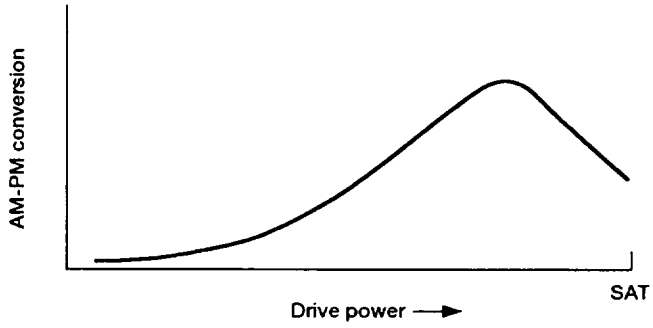

(b) AM-PM conversion.

Figure 3.—Effect of drive power on phase linearity.

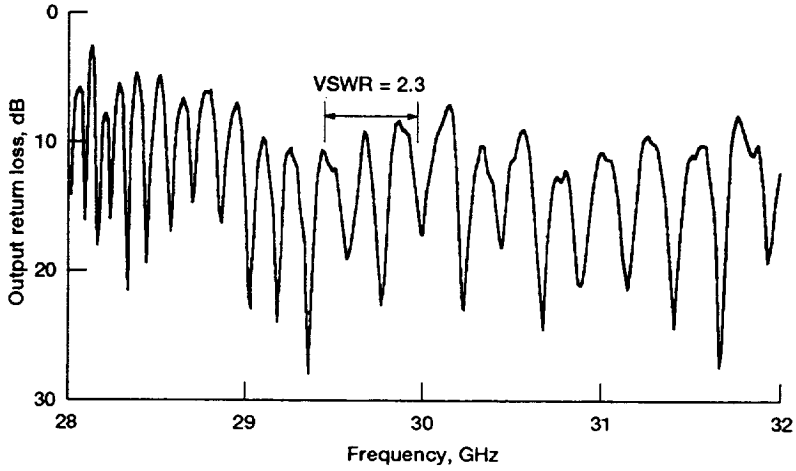

Figure 4.—Tube 1 output reflection cold test.

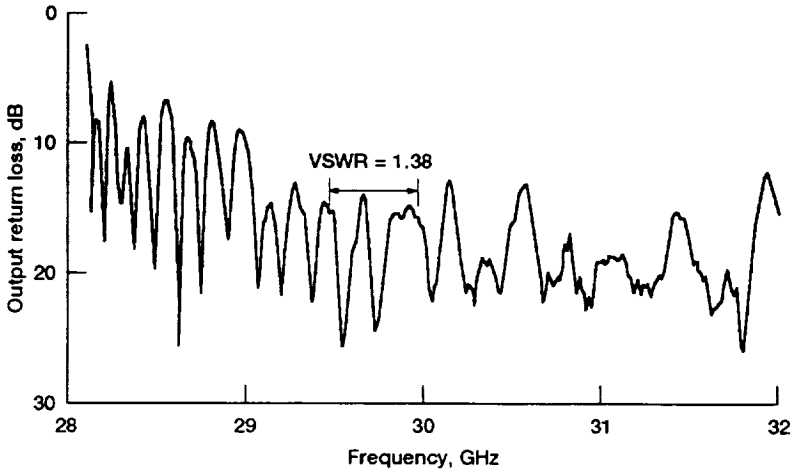

Figure 5.—Tube 2 output reflection cold test.

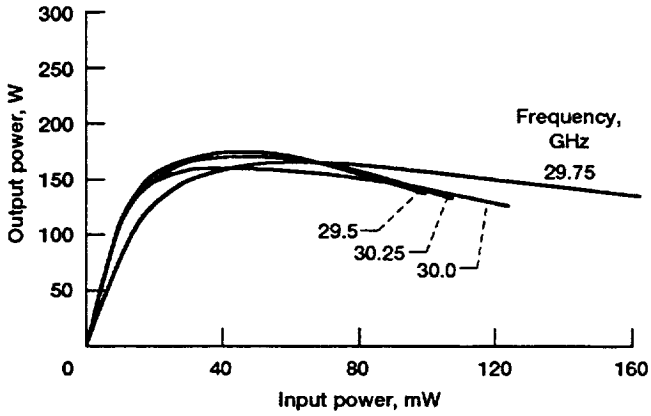

Figure 6.—Transfer characteristics of tube 2 at 16.0-kV level.

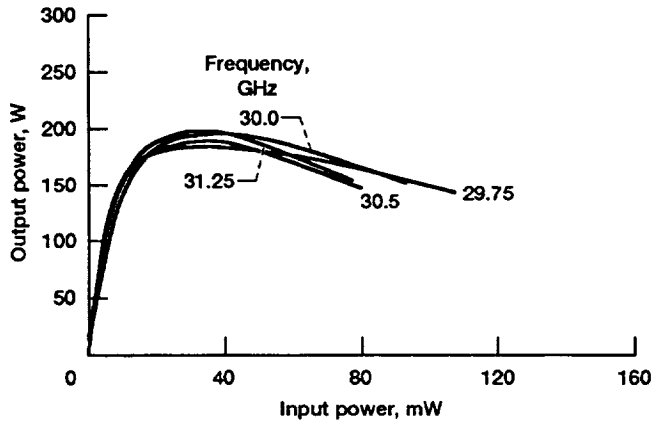

Figure 7.—Transfer characteristics of tube 2 at 16.25-kV level.

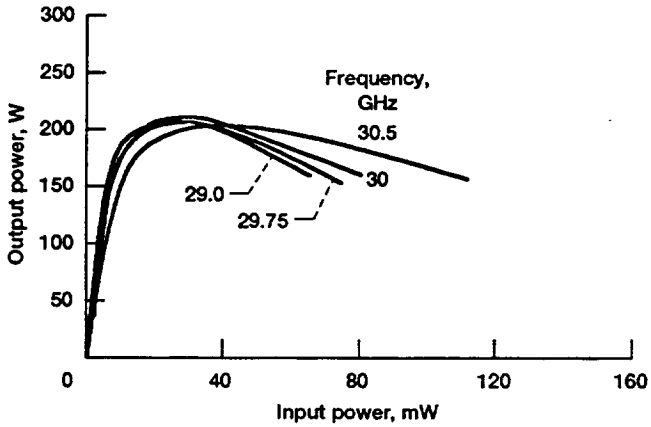

Figure 8.—Transfer characteristics of tube 2 at 16.5-kV level.

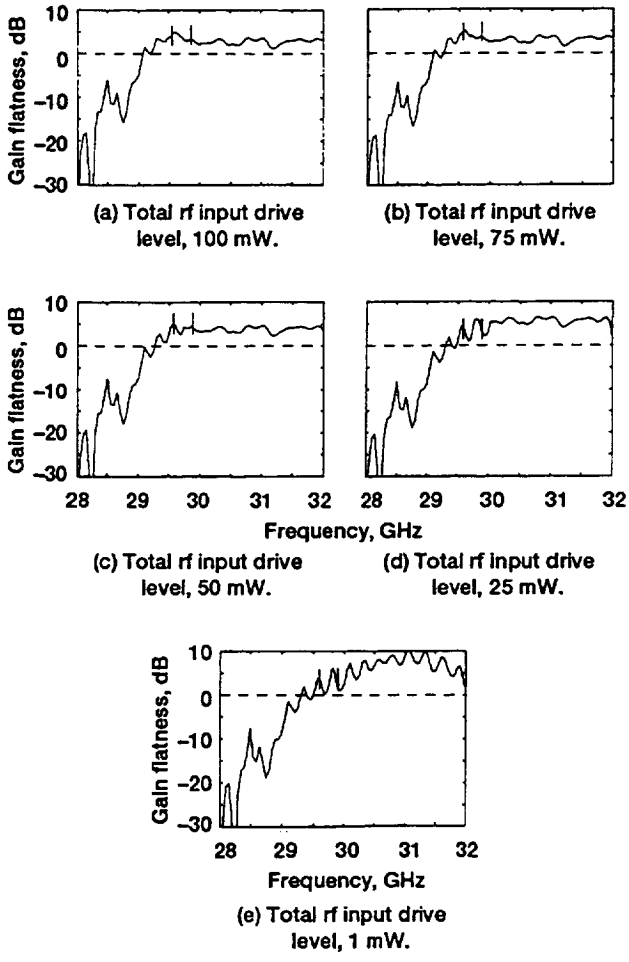

Figure 9.—Continuous wave performance of tube 1.

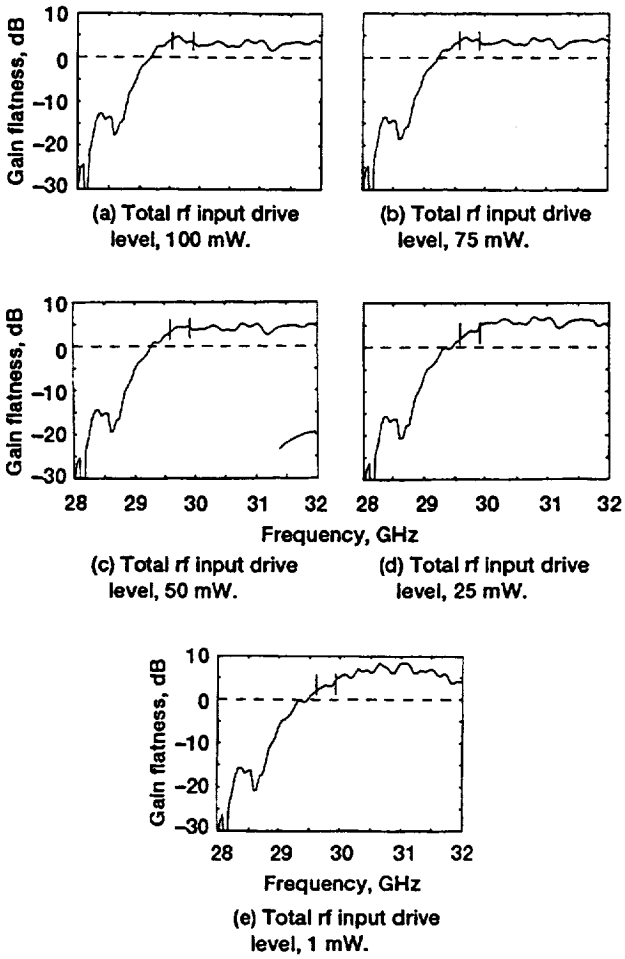

Figure 10.—Continuous wave performance of tube 2.

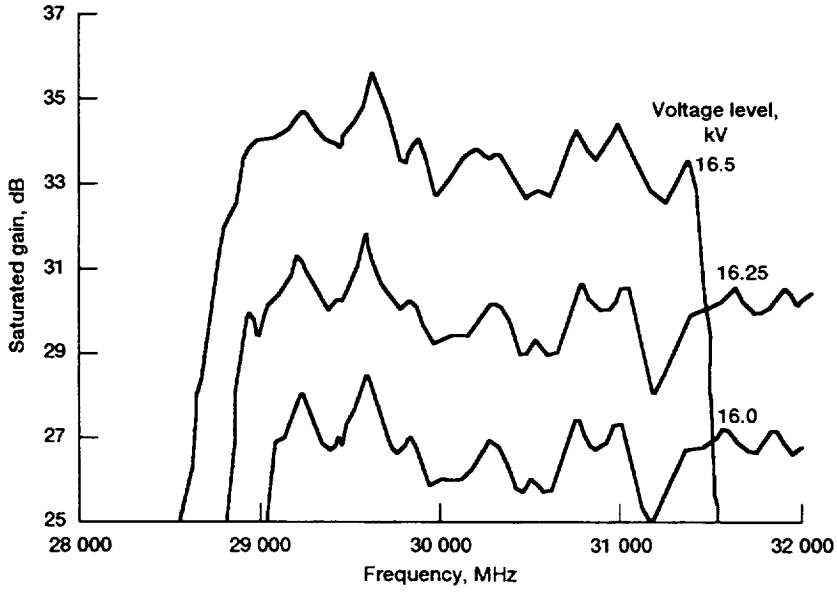

Figure 11.—Tube 1 saturated gain versus frequency at three voltages.

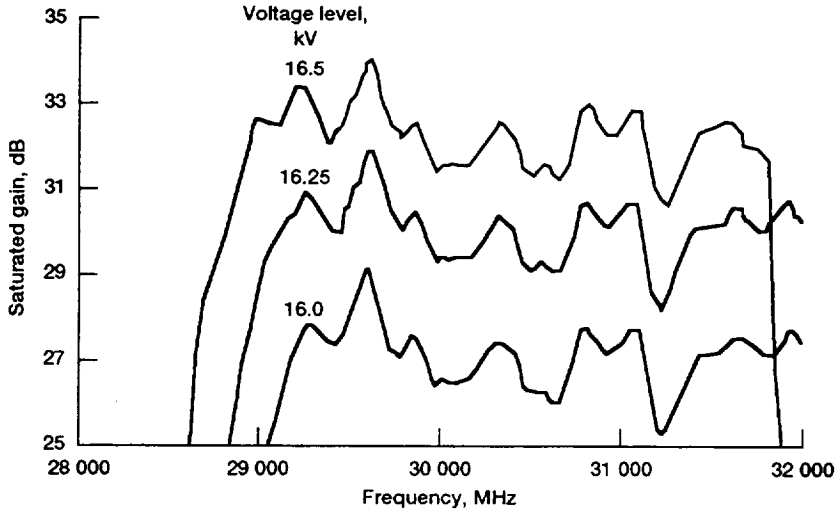

Figure 12.—Tube 2 saturated gain versus frequency at three voltages.

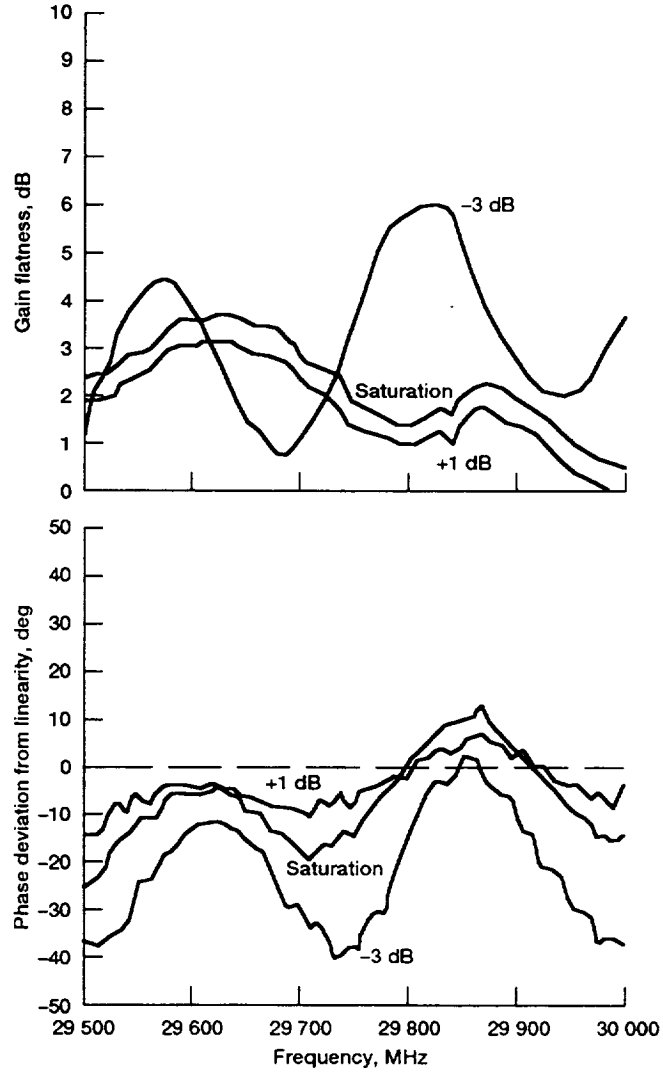

Figure 13.—Relationship of gain flatness to phase deviation close to saturation in tube 1 at 16.0 kV.

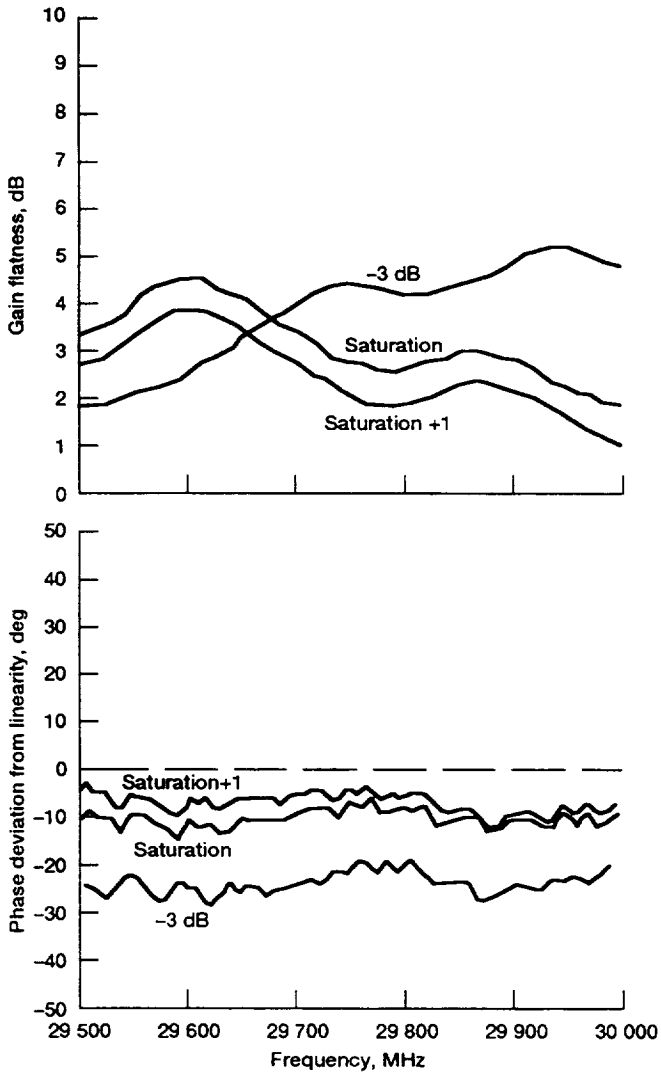

Figure 14.—Relationship of gain flatness to phase deviation close to saturation in tube 2 at 16.0 kV.

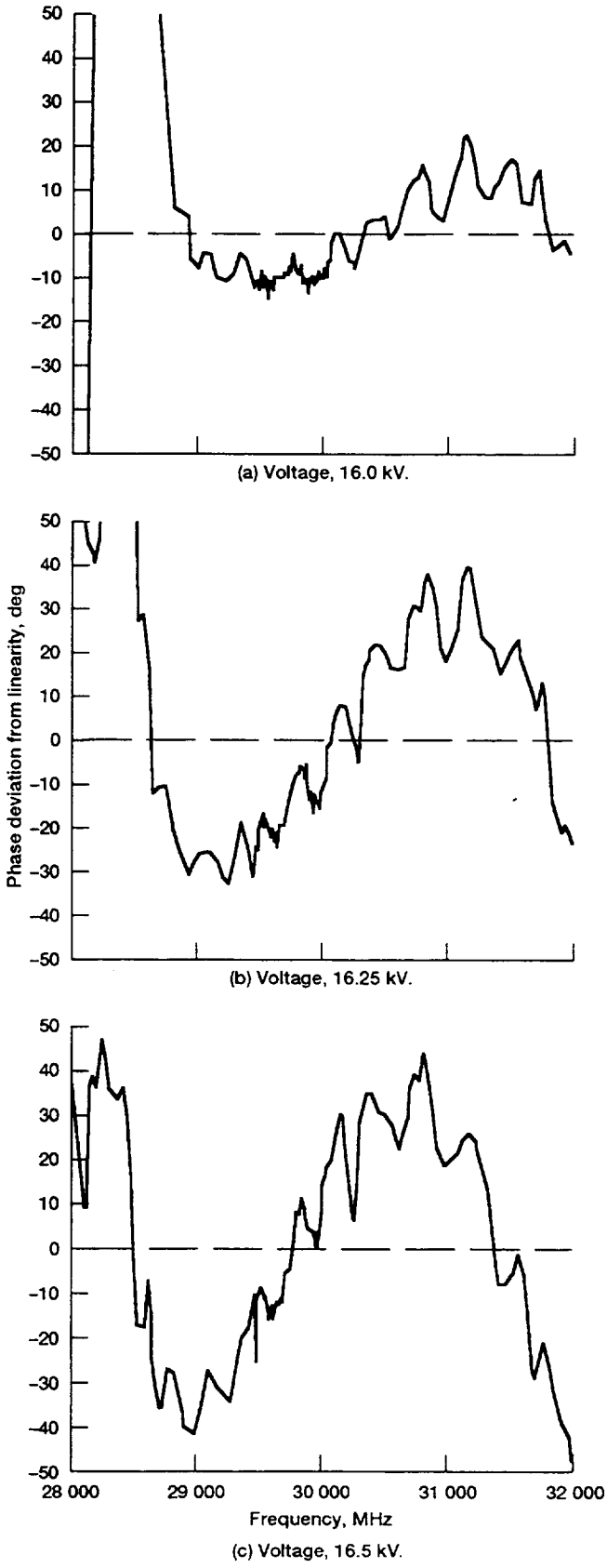

(a) Voltage, 16.0 kV.

(b) Voltage, 16.25 kV.

(c) Voltage, 16.5 kV.

Figure 15.—Difference in phase linearity at saturation in tube 2 for three voltages.

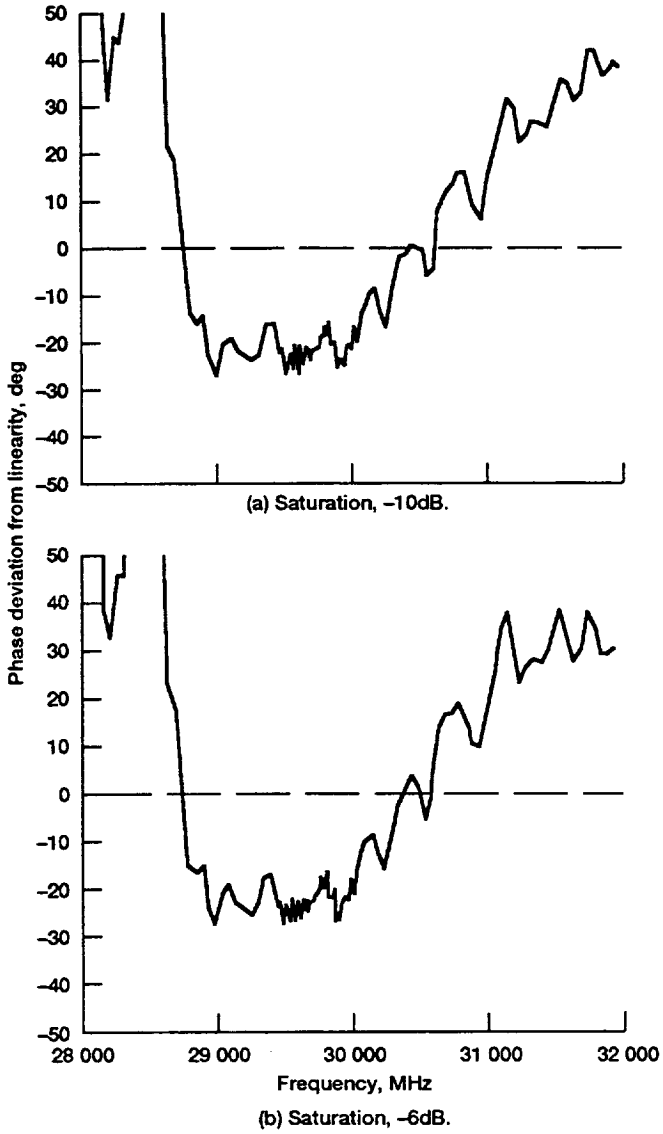

(a) Saturation, –10dB.

(b) Saturation, –6dB.

Figure 16.—Phase deviation at two levels in the linear region in tube 2.

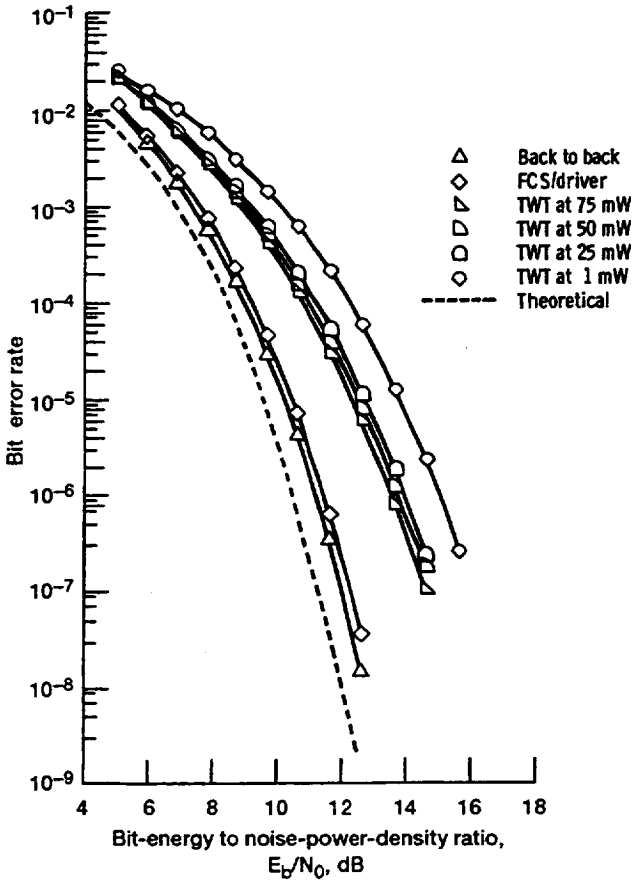

Figure 17.—Tube 1 bit-error-rate performance.

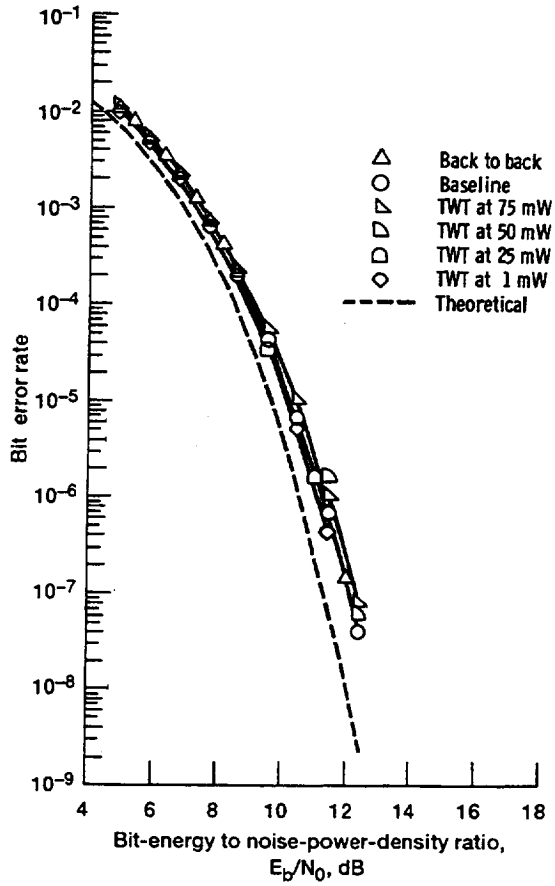

Figure 18.—Tube 2 bit-error-rate performance.

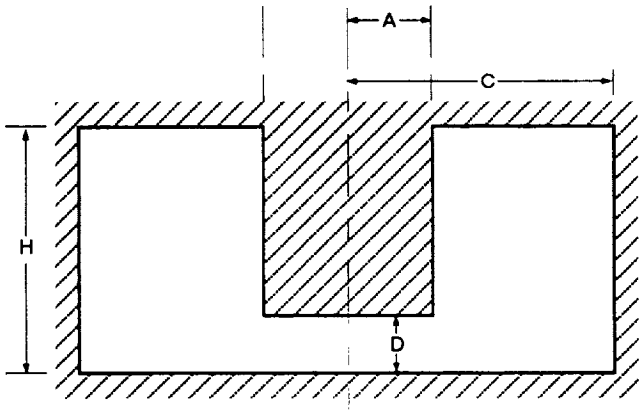

Dimension, mm	Frequency change, ΔF, GHz/mm
A 0.77	-11.00
C 2.20	-17.16
D 0.50	+50.70
H 1.28	-30.00

Figure 19.—Design of 30-GHz re-entrant cavity.

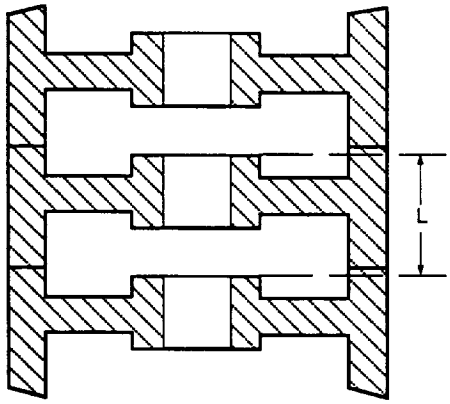

(a) Double re-entrant Hughes cavity (A).

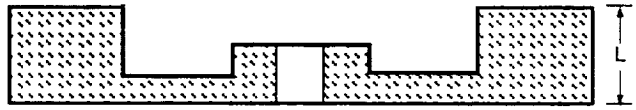

(b) Simple single re-entrant cavity (B).

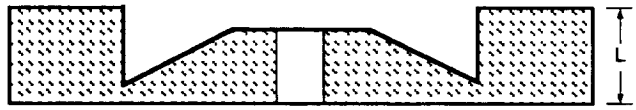

(c) Truncated-cone, single re-entrant cavity for increased ruggedness (C).

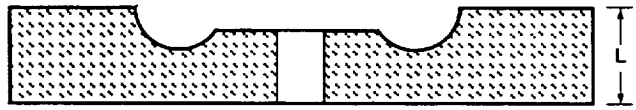

(d) Cusp design, single re-entrant cavity for increased ruggedness, improved thermal capacity, and ease of manufacture (D).

Figure 20.—Circuit cavity designs for use in coupled-cavity traveling wave tubes.

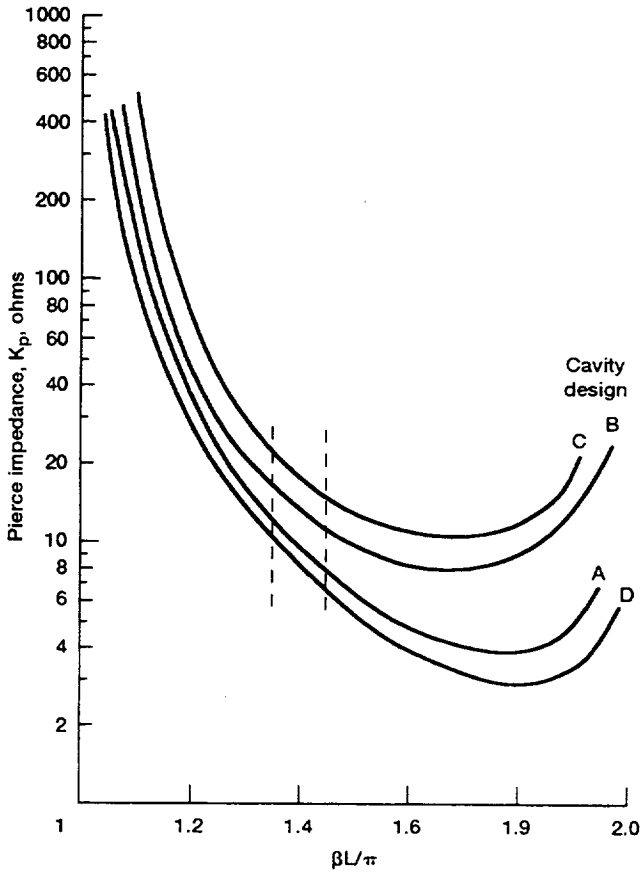

Figure 21.—Impedance of four circuit designs.

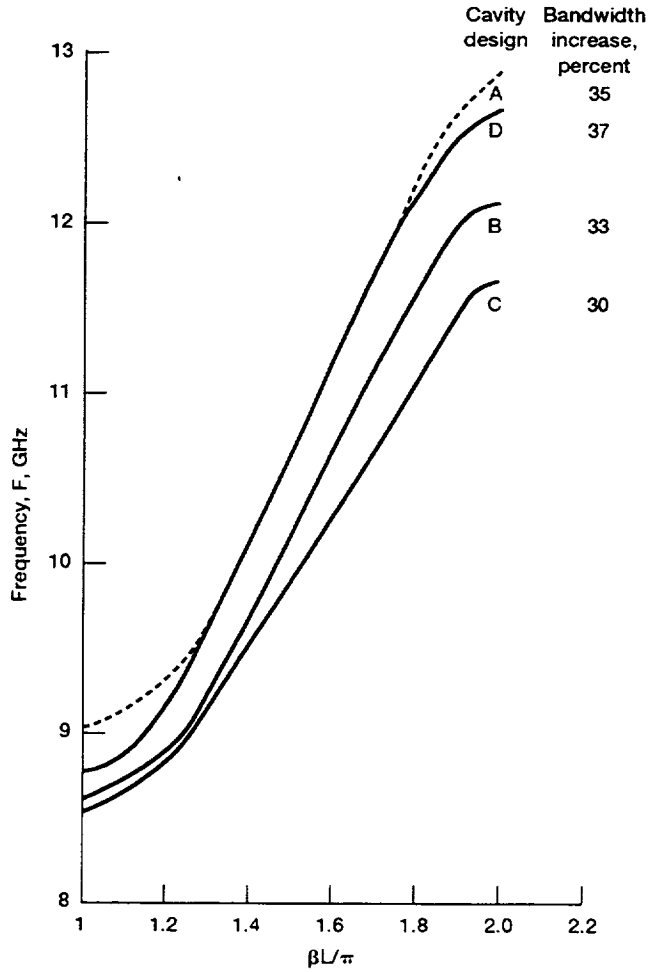

Figure 22.—Circuit bandwidth.

APPENDIX — PHASE DEVIATION FROM LINEARITY IN SATURATED AND LINEAR REGIONS OF 914H COUPLED-CAVITY TRAVELING WAVE TUBE

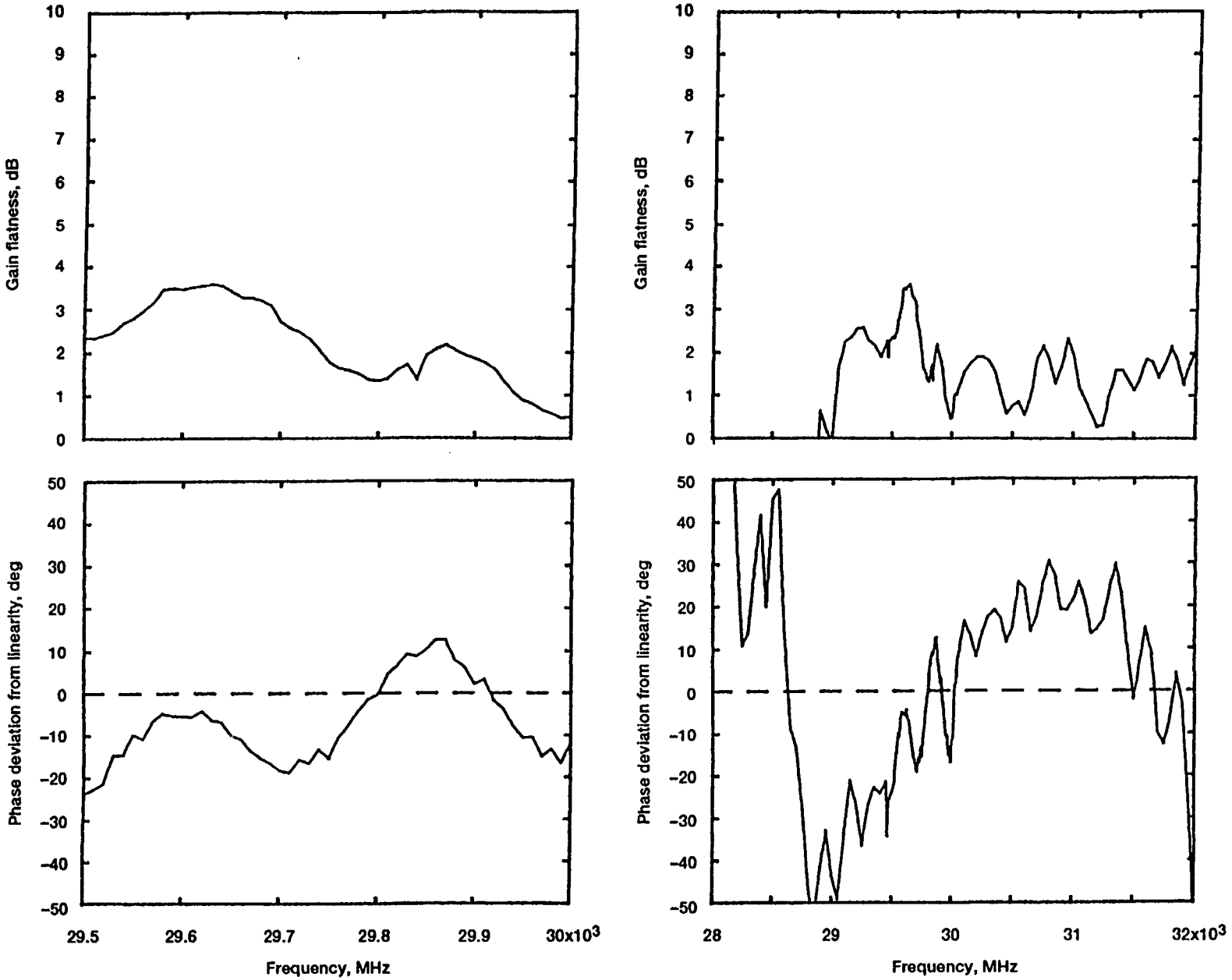

Figure 23.—Relationship of gain flatness to phase deviation from linearity for tube 1 at 16.0 kV and saturation.

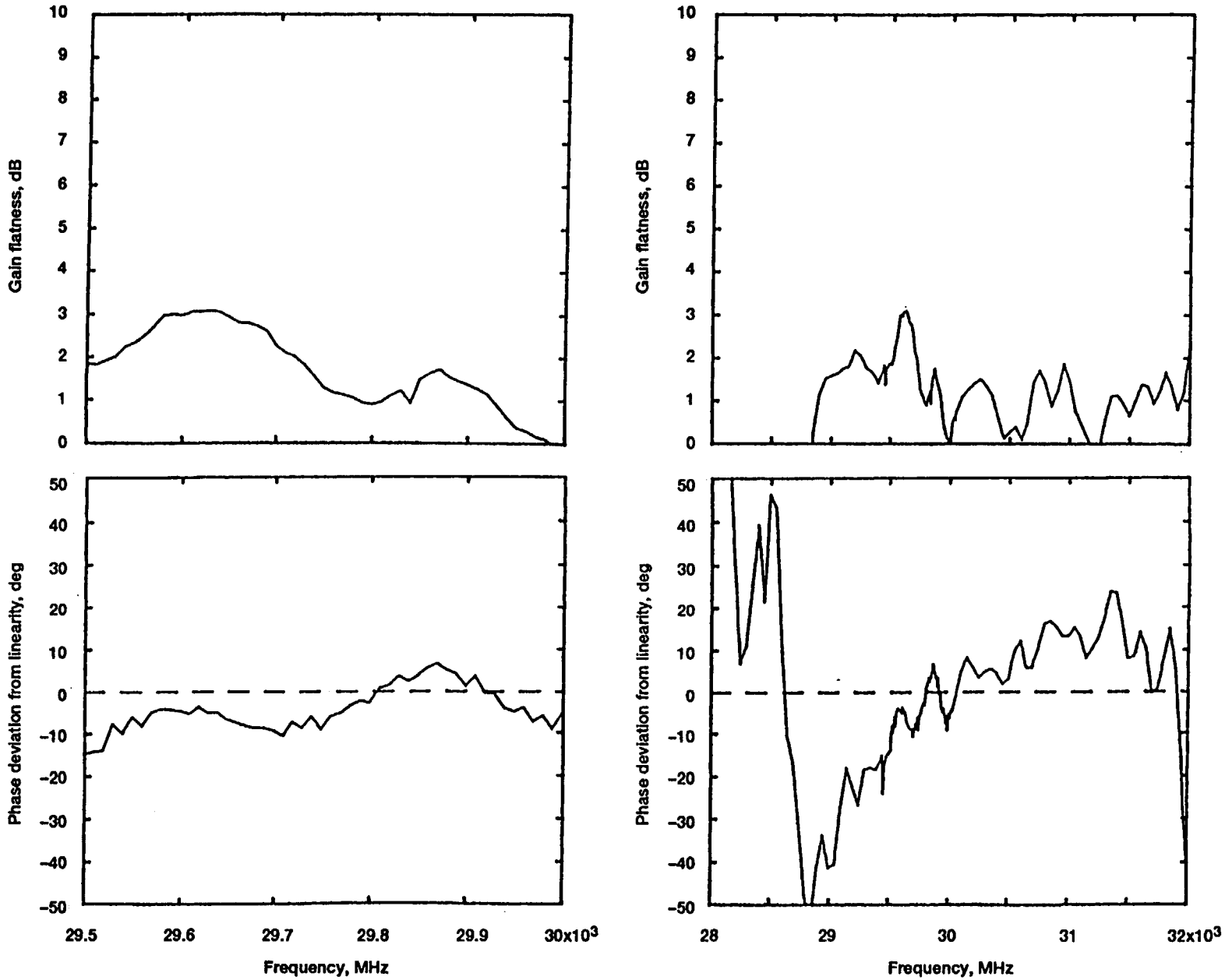

Figure 24.—Relationship of gain flatness to phase deviation from linearity for tube 1 at 16.0 kV and saturation +1 dB.

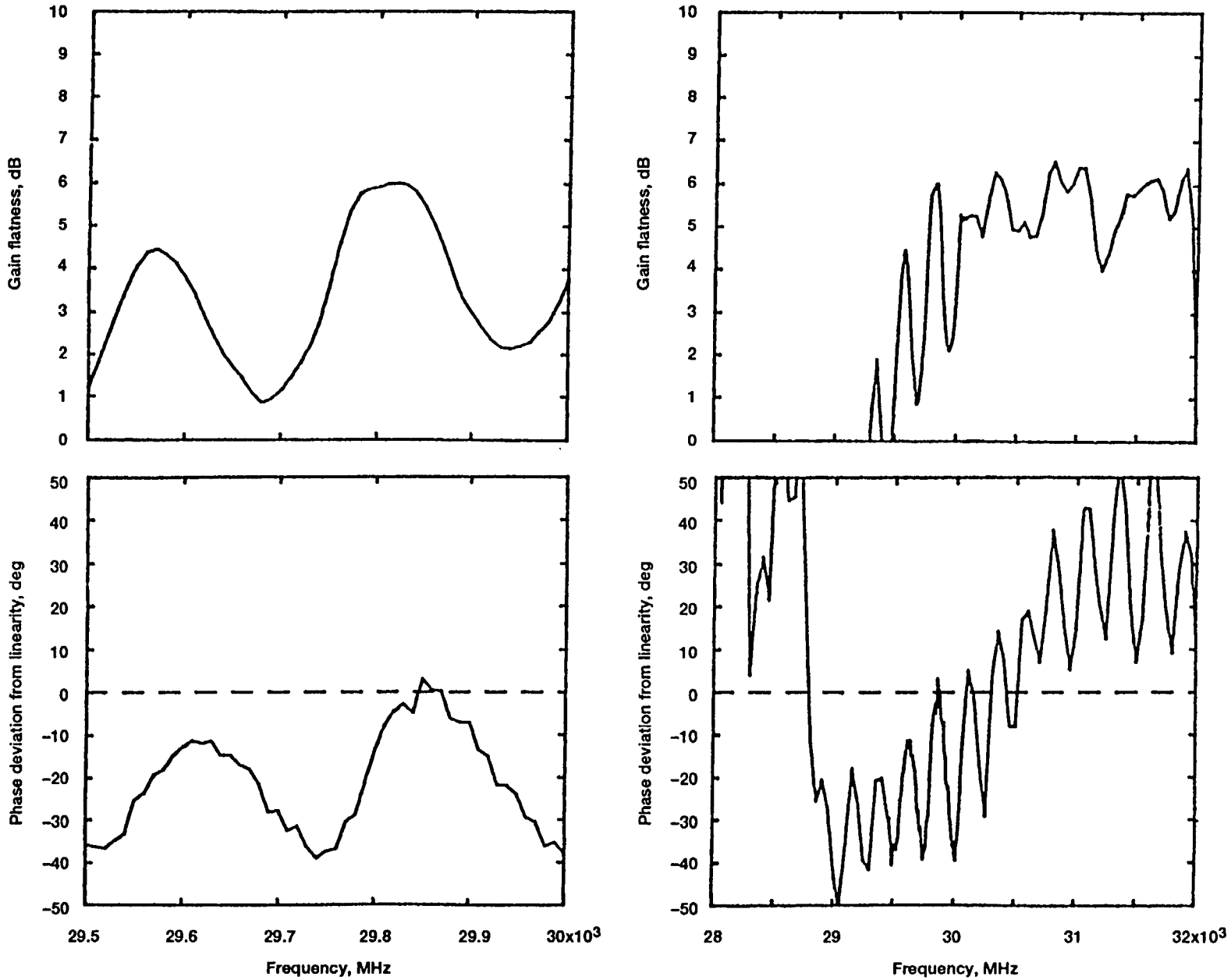

Figure 25.—Relationship of gain flatness to phase deviation from linearity for tube 1 at 16.0 kV and saturation –3 dB.

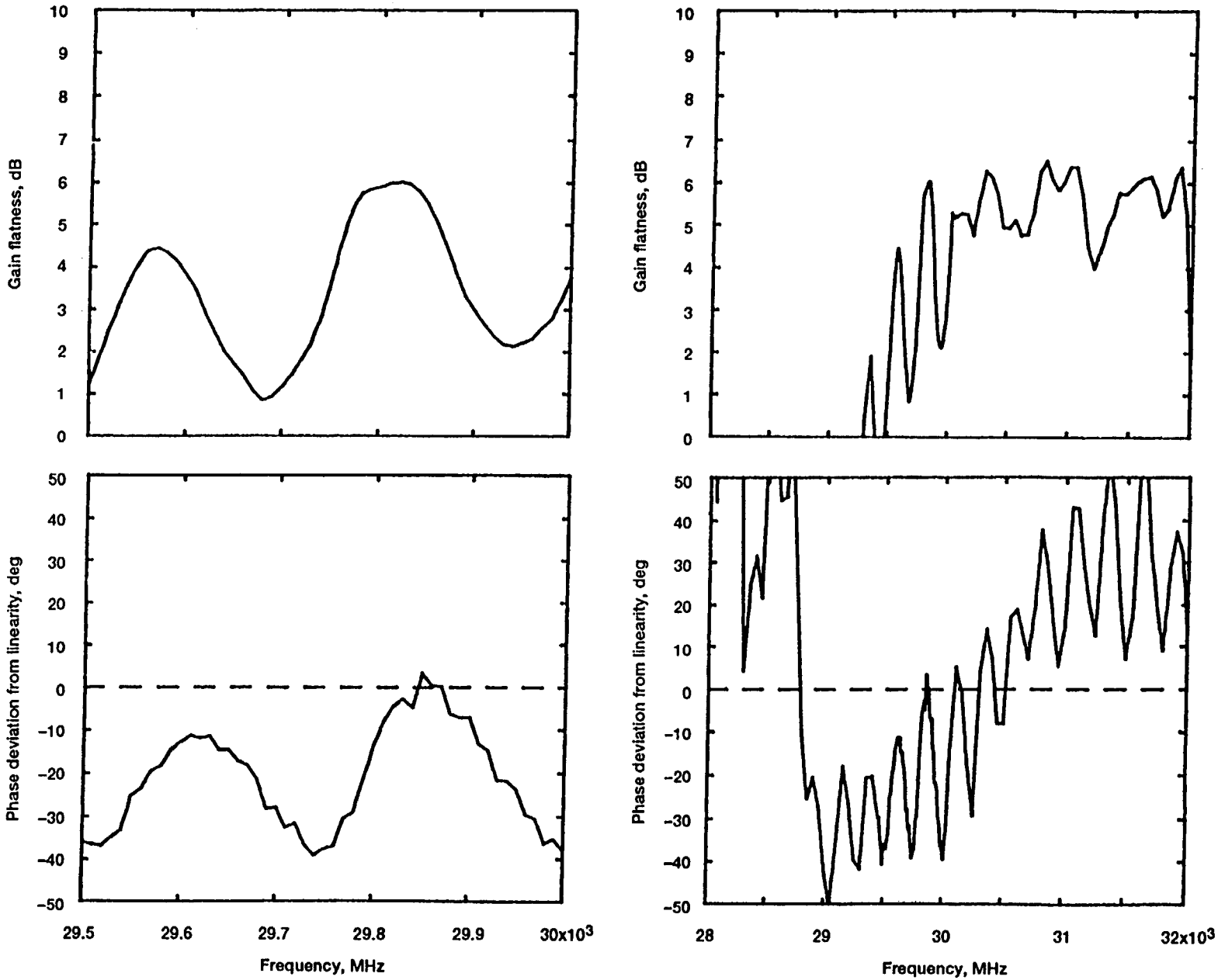

Figure 26.—Relationship of gain flatness to phase deviation from linearity for tube 1 at 16.0 kV and saturation -6 dB.

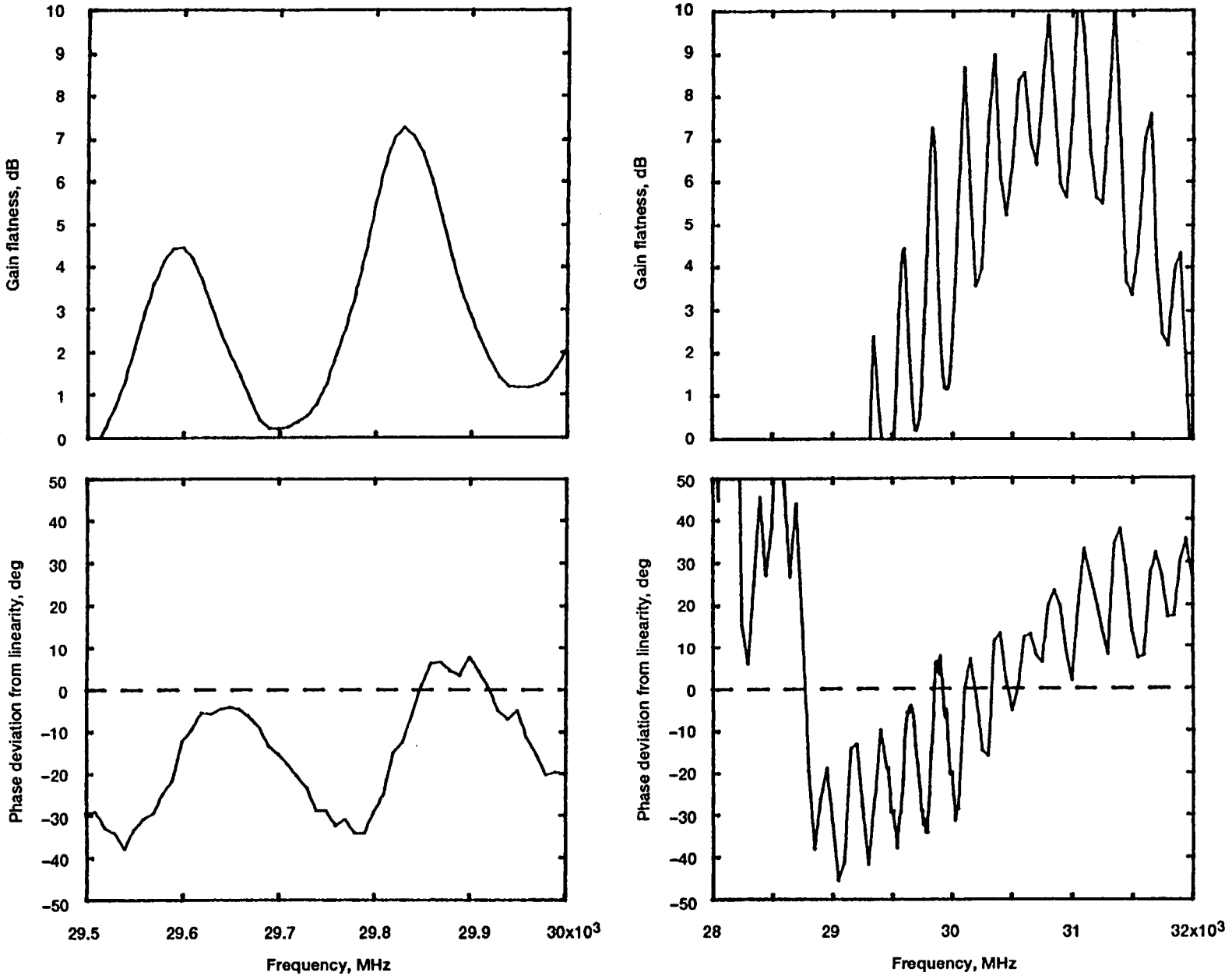

Figure 27.—Relationship of gain flatness to phase deviation from linearity for tube 1 at 16.0 kV and saturation -10 dB.

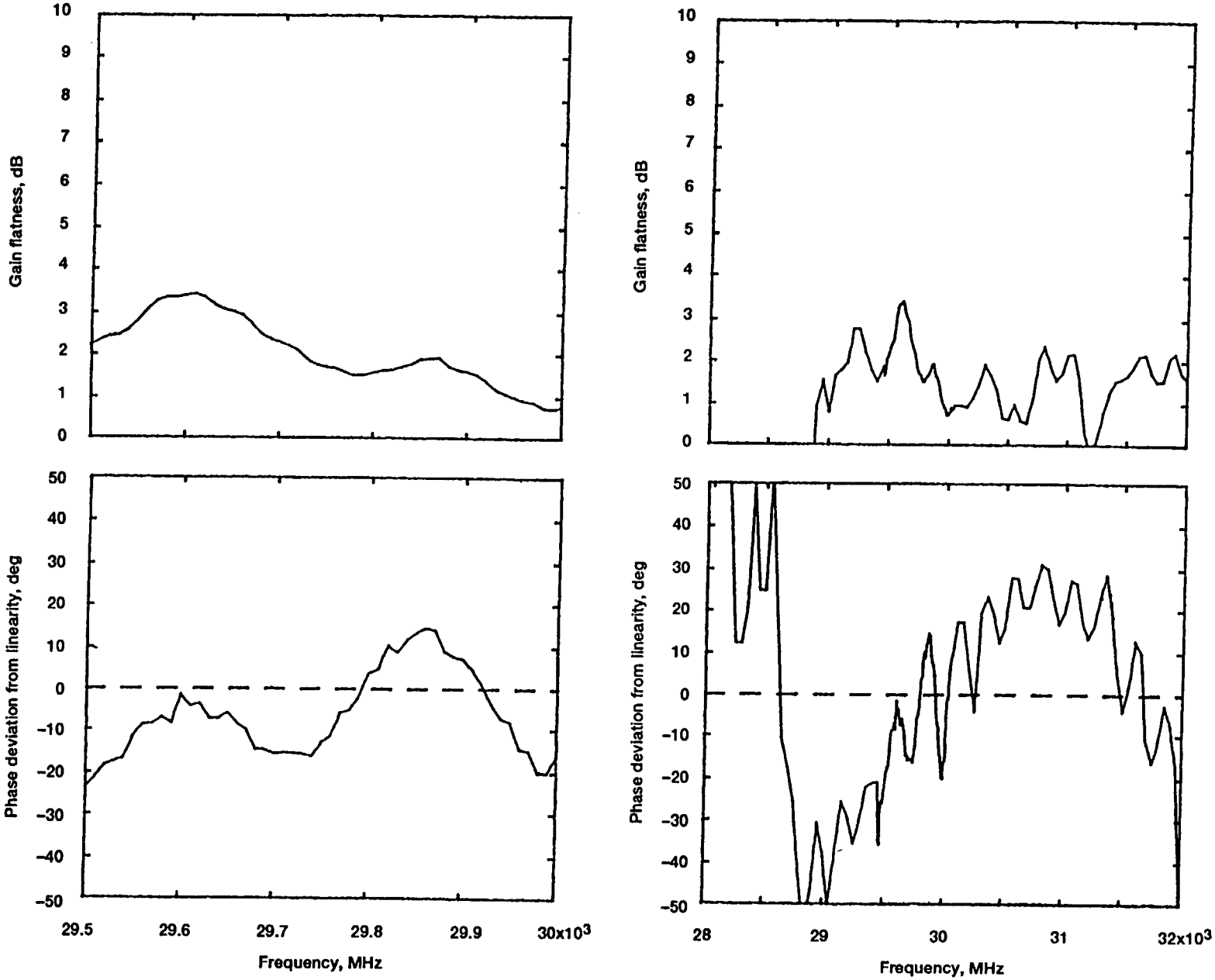

Figure 28.—Relationship of gain flatness to phase deviation from linearity for tube 1 at 16.25 kV and saturation.

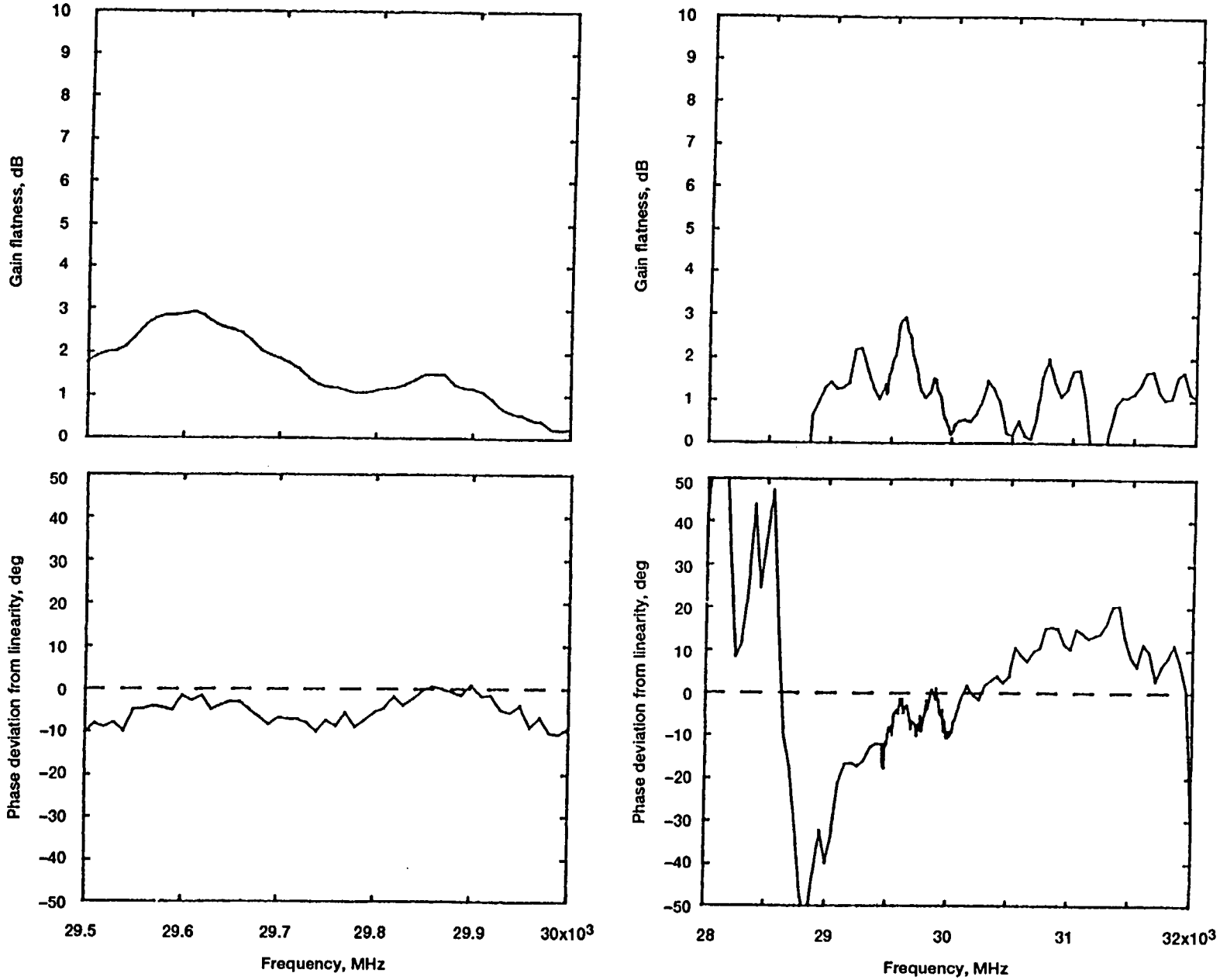

Figure 29.—Relationship of gain flatness to phase deviation from linearity for tube 1 at 16.25 kV and saturation +1 dB.

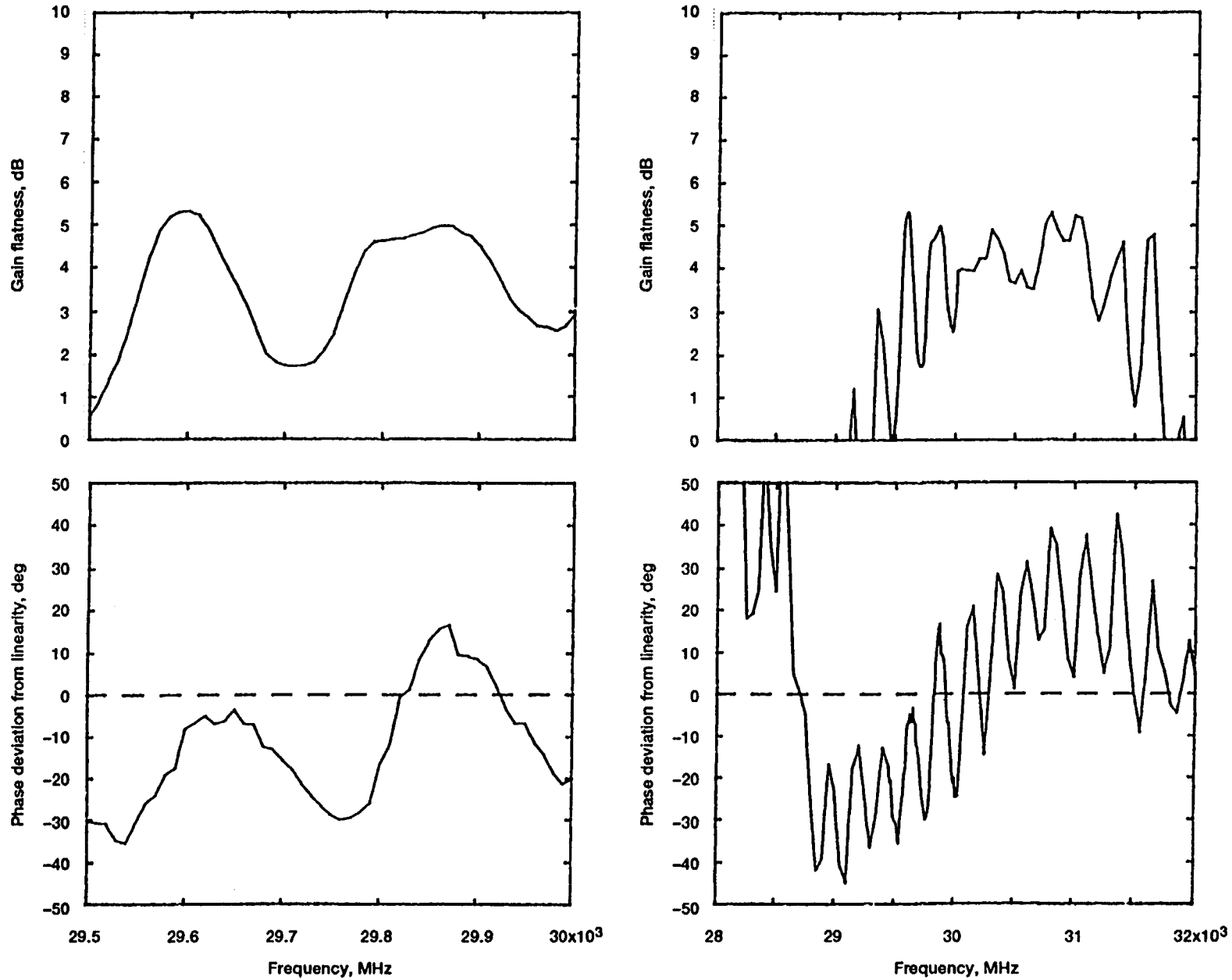

Figure 30.—Relationship of gain flatness to phase deviation from linearity for tube 1 at 16.25 kV and saturation –3 dB.

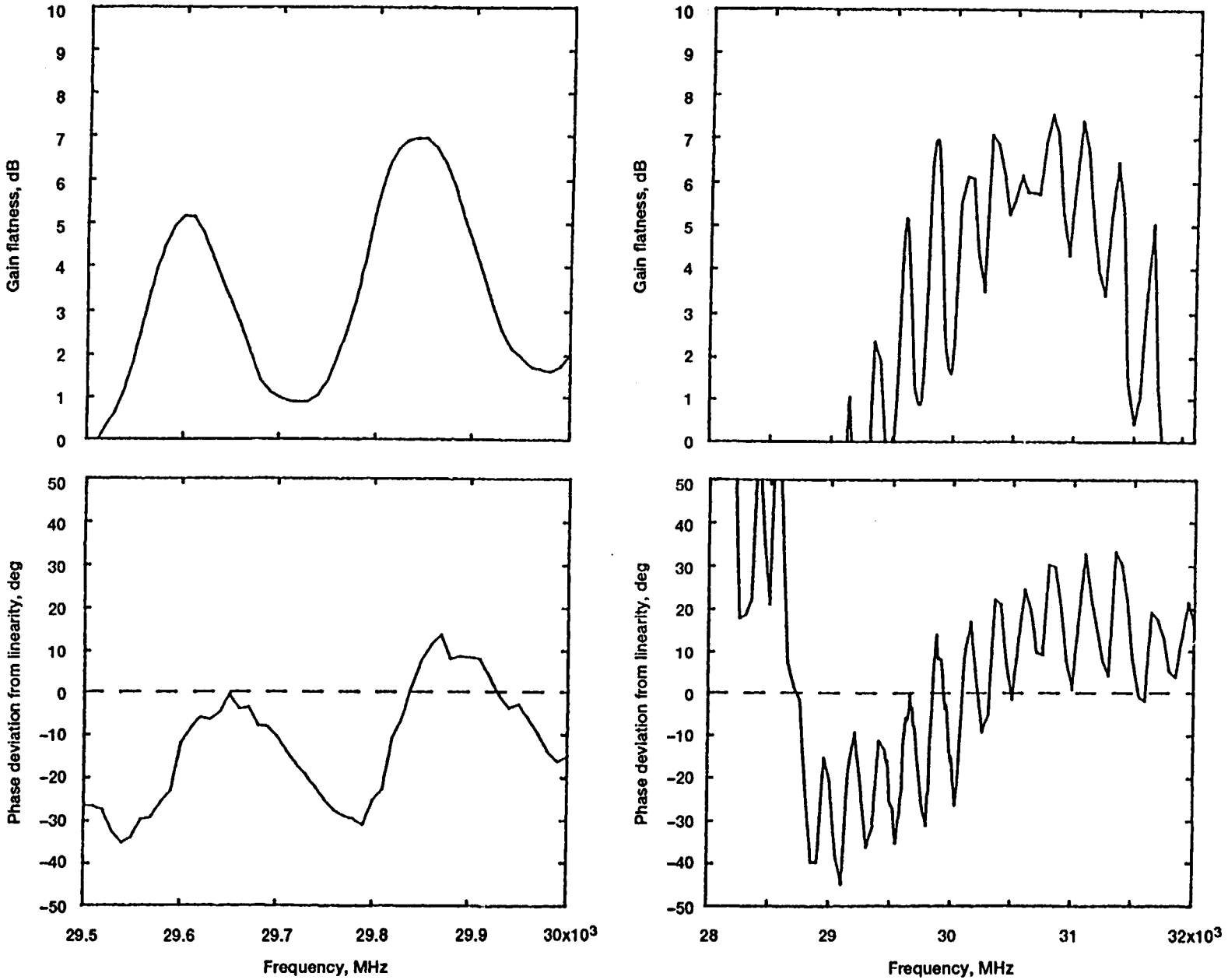

Figure 31.—Relationship of gain flatness to phase deviation from linearity for tube 1 at 16.25 kV and saturation –6 dB.

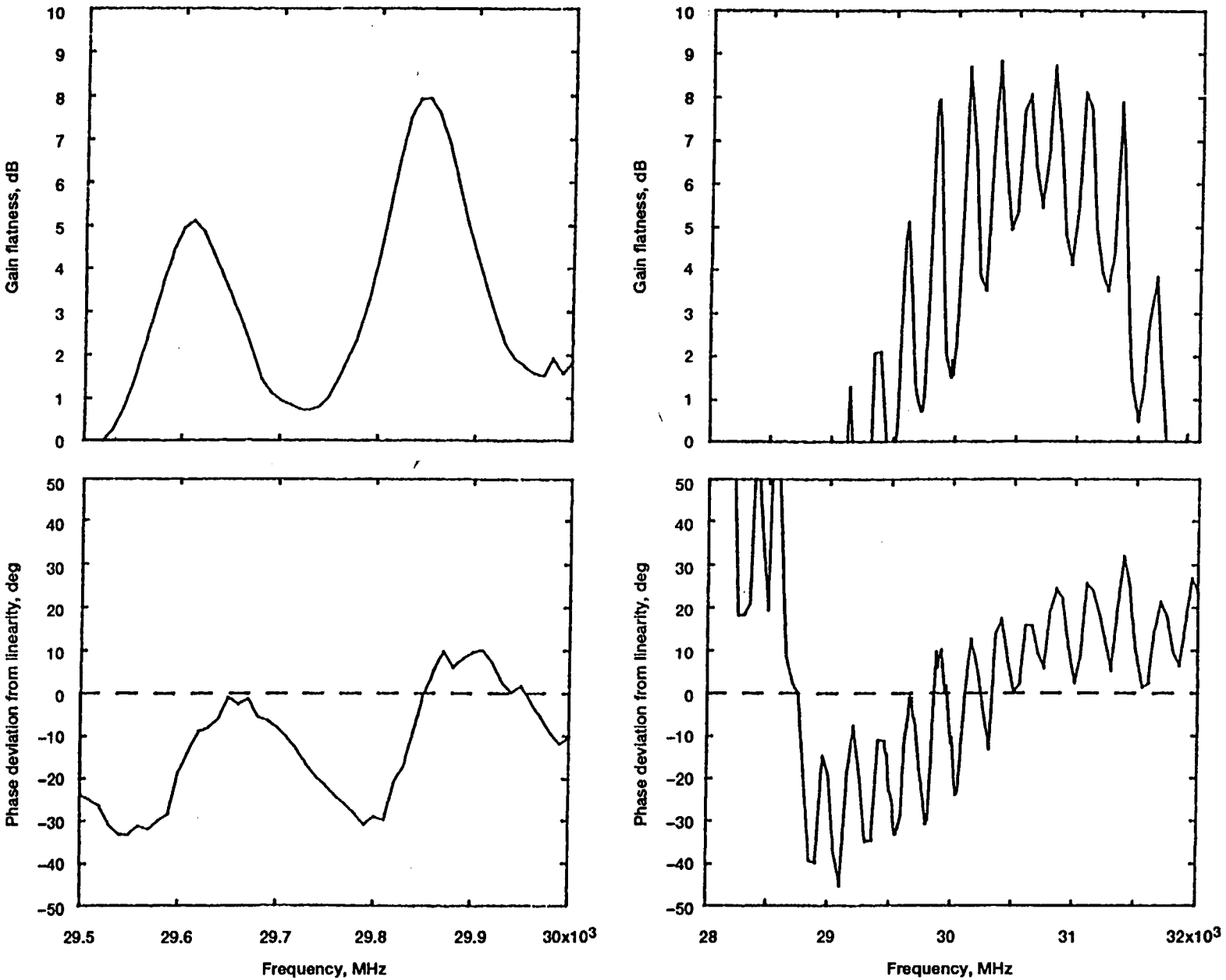

Figure 32.—Relationship of gain flatness to phase deviation from linearity for tube 1 at 16.25 kV and saturation –10 dB.

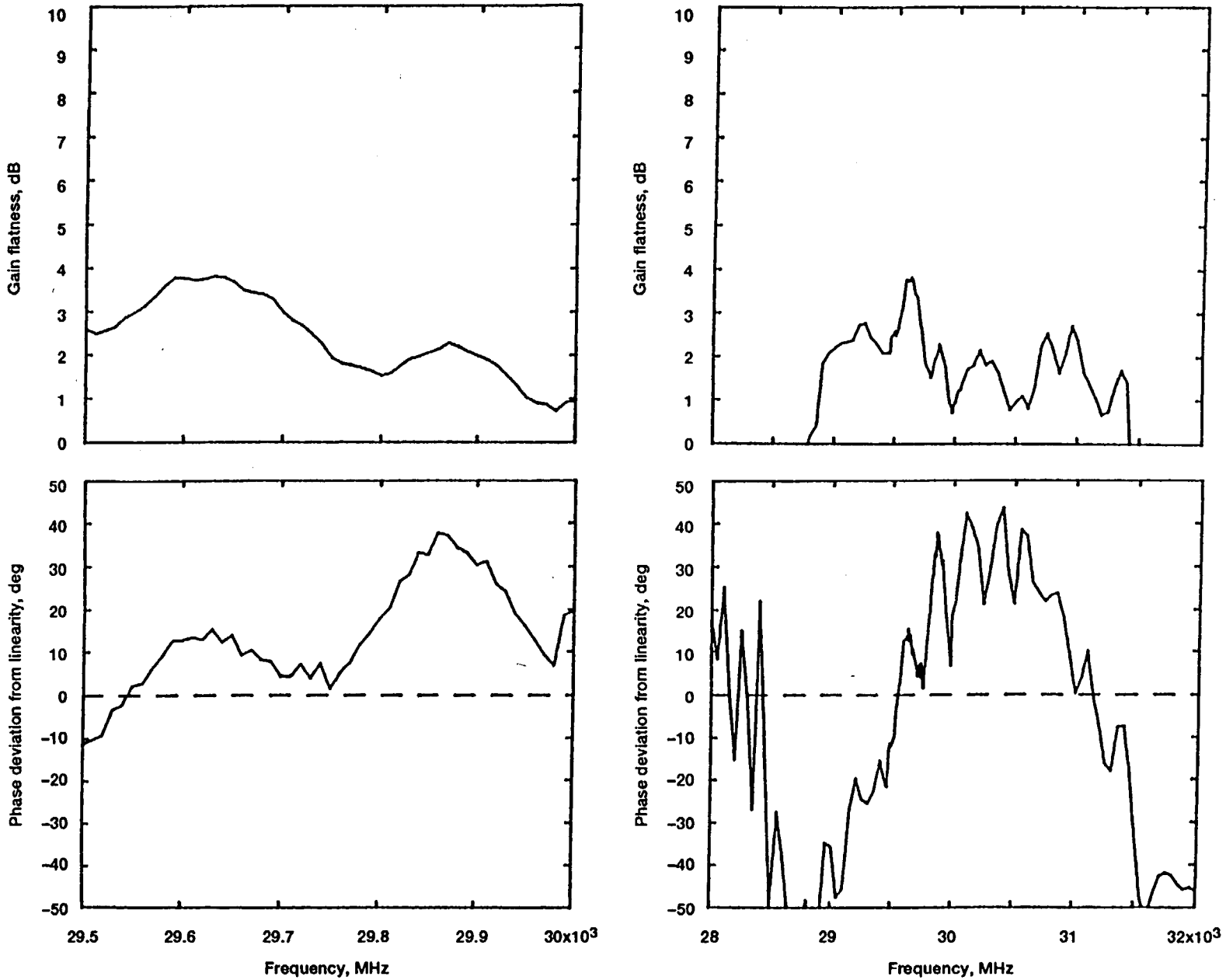

Figure 33.—Relationship of gain flatness to phase deviation from linearity for tube 1 at 16.5 kV and saturation.

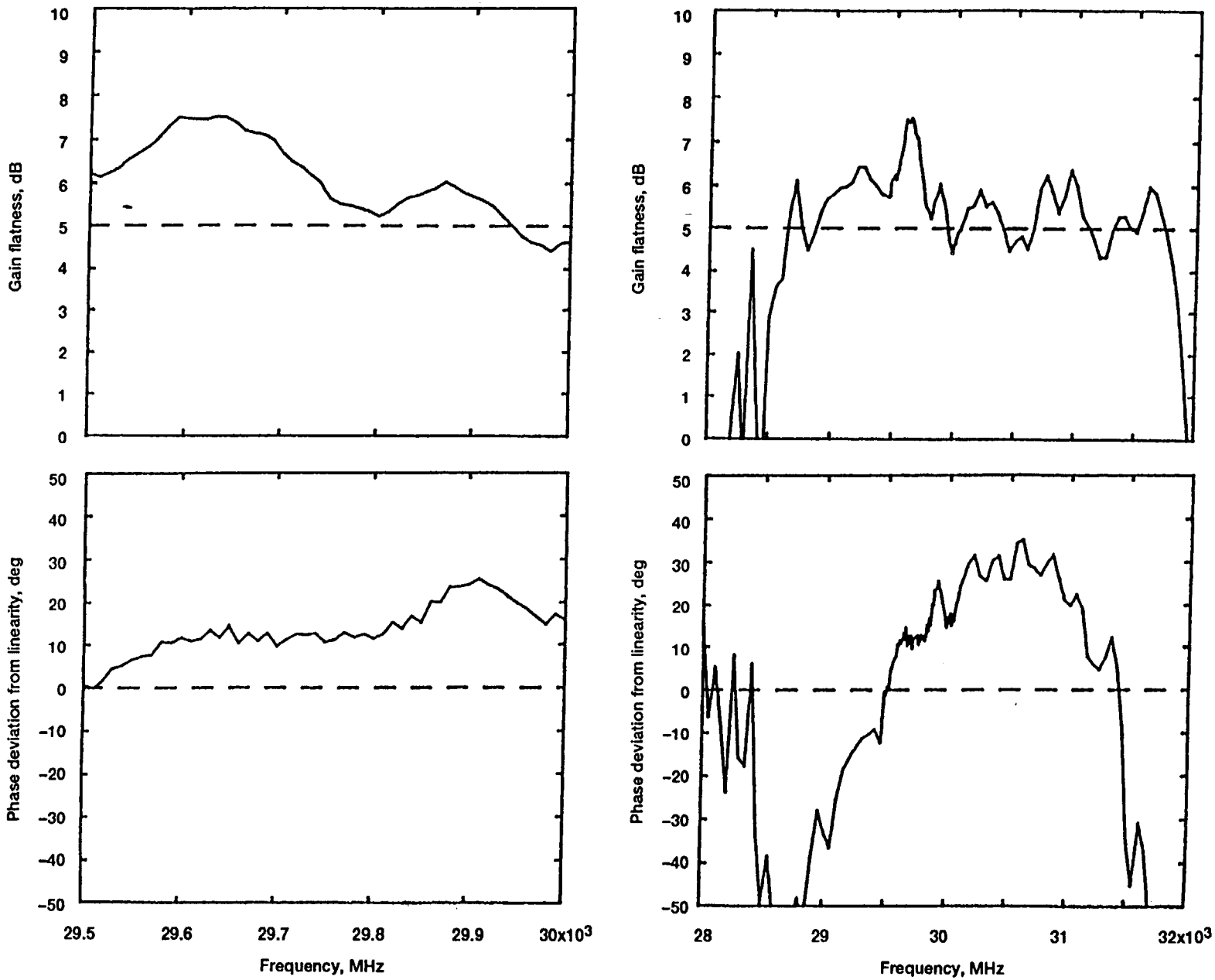

Figure 34.—Relationship of gain flatness to phase deviation from linearity for tube 1 at 16.5 kV and saturation +1 dB.

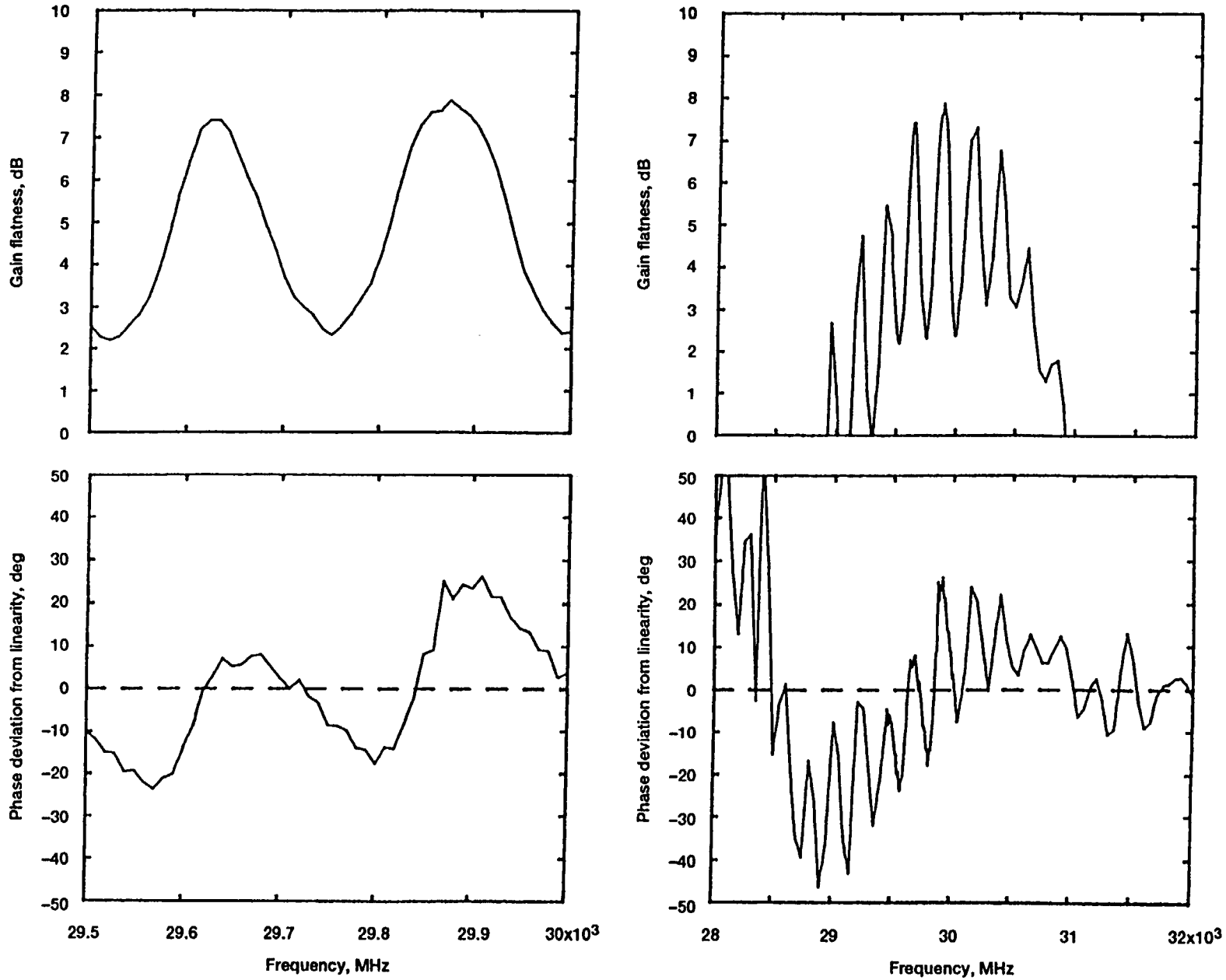

Figure 35.—Relationship of gain flatness to phase deviation from linearity for tube 1 at 16.5 kV and saturation –3 dB.

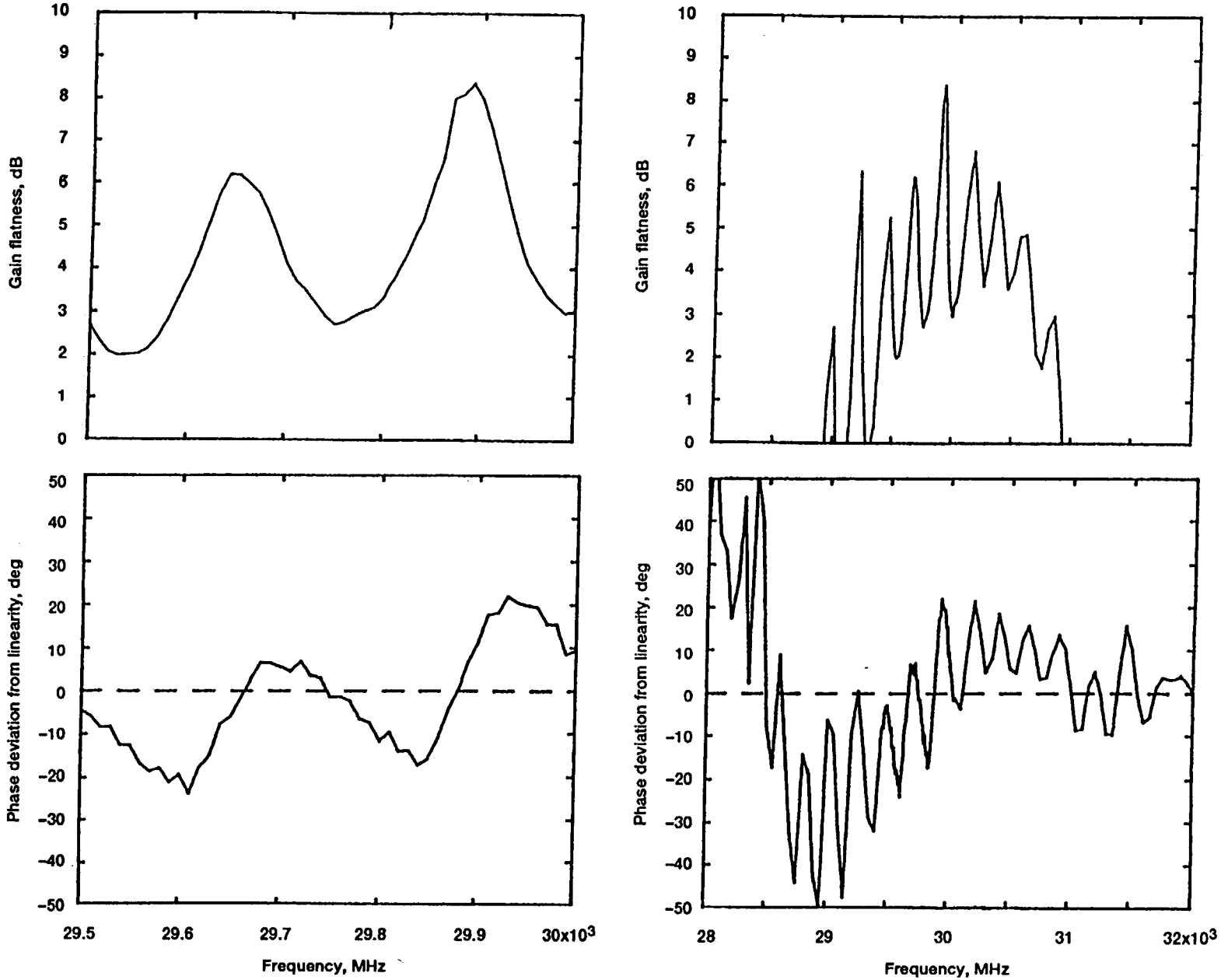

Figure 36.—Relationship of gain flatness to phase deviation from linearity for tube 1 at 16.5 kV and saturation –6 dB.

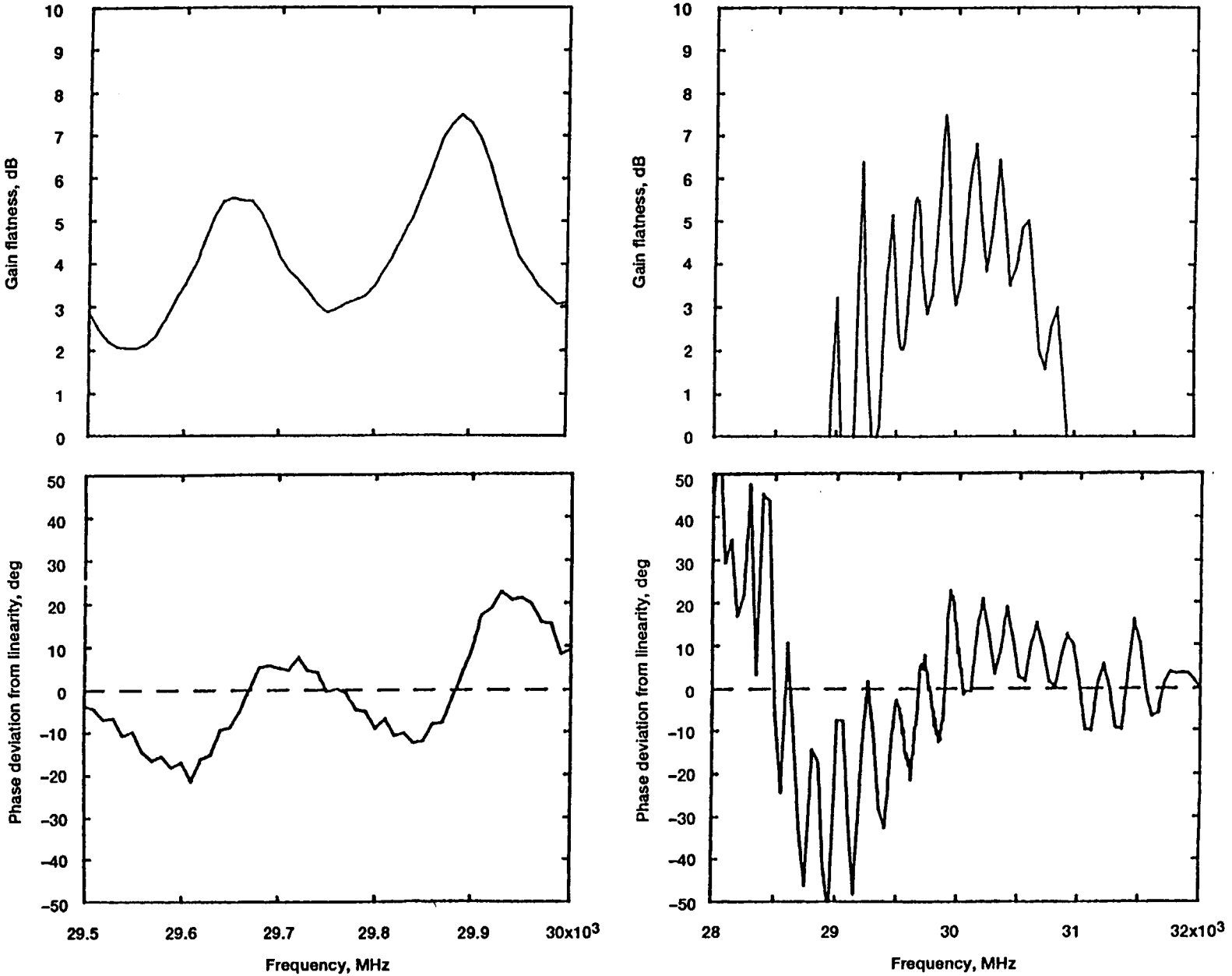

Figure 37.—Relationship of gain flatness to phase deviation from linearity for tube 1 at 16.5 kV and saturation -10 dB.

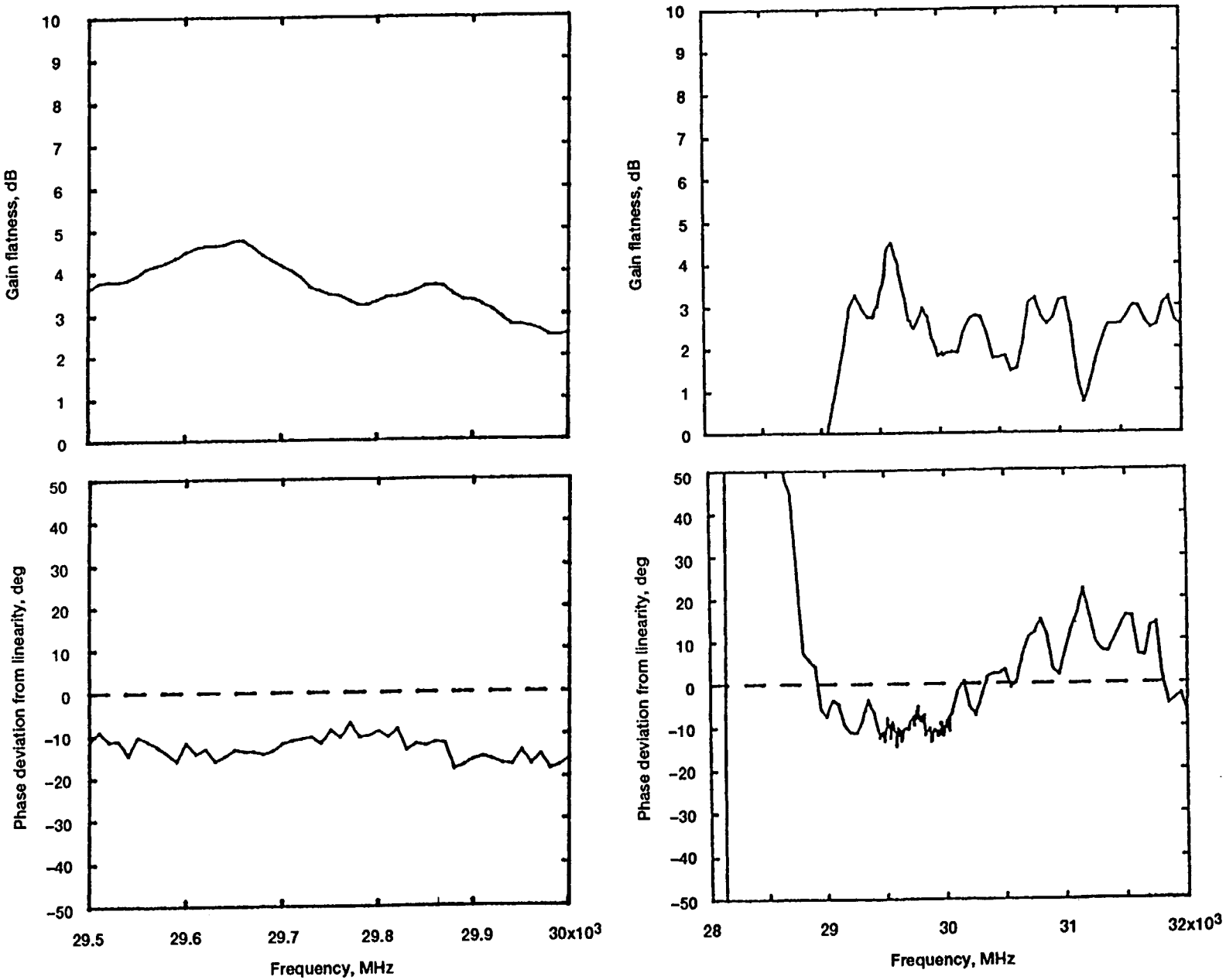

Figure 38.—Relationship of gain flatness to phase deviation from linearity for tube 2 at 16.0 kV and saturation.

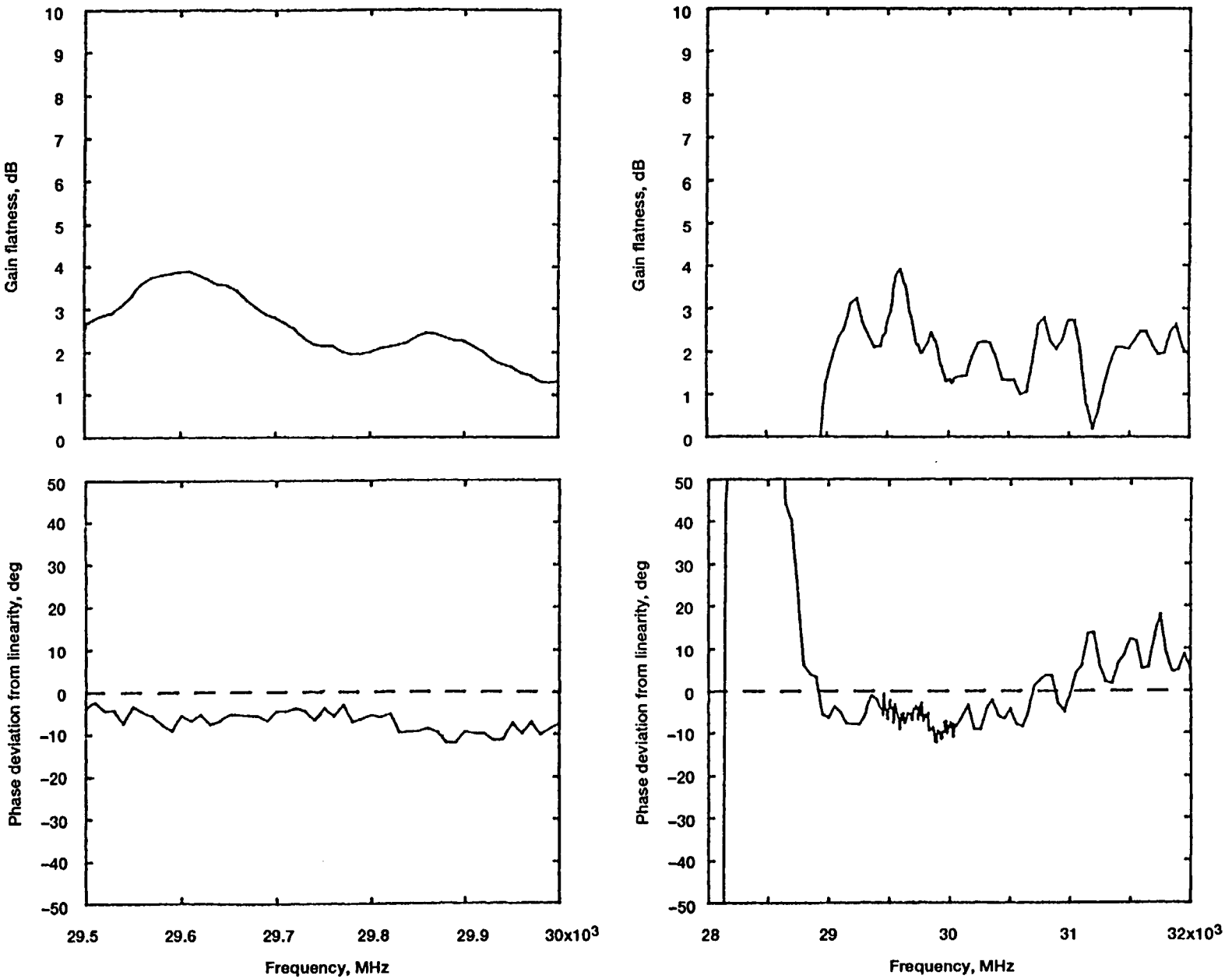

Figure 39.—Relationship of gain flatness to phase deviation from linearity for tube 2 at 16.0 kV and saturation +1 dB.

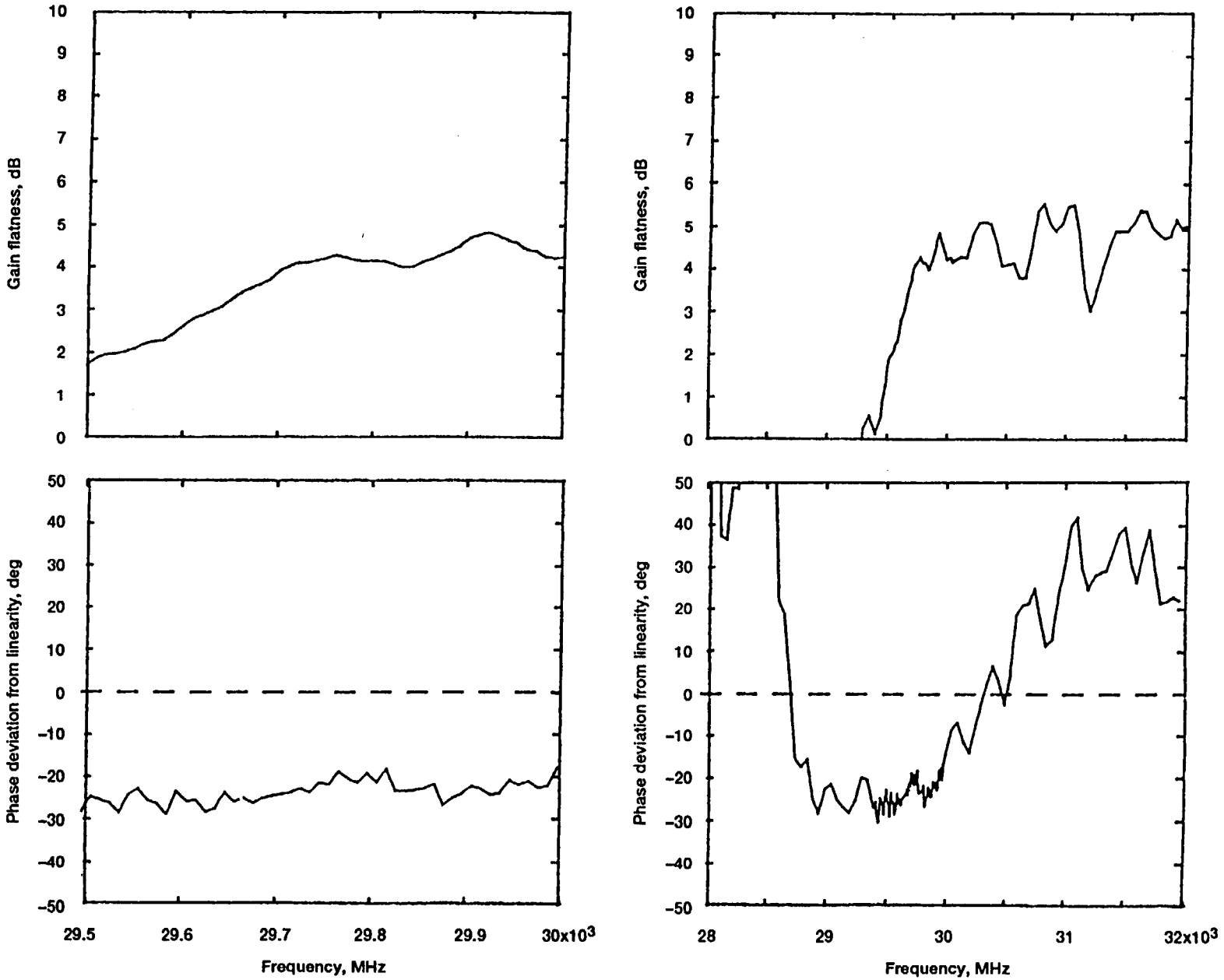

Figure 40.—Relationship of gain flatness to phase deviation from linearity for tube 2 at 16.0 kV and saturation –3 dB.

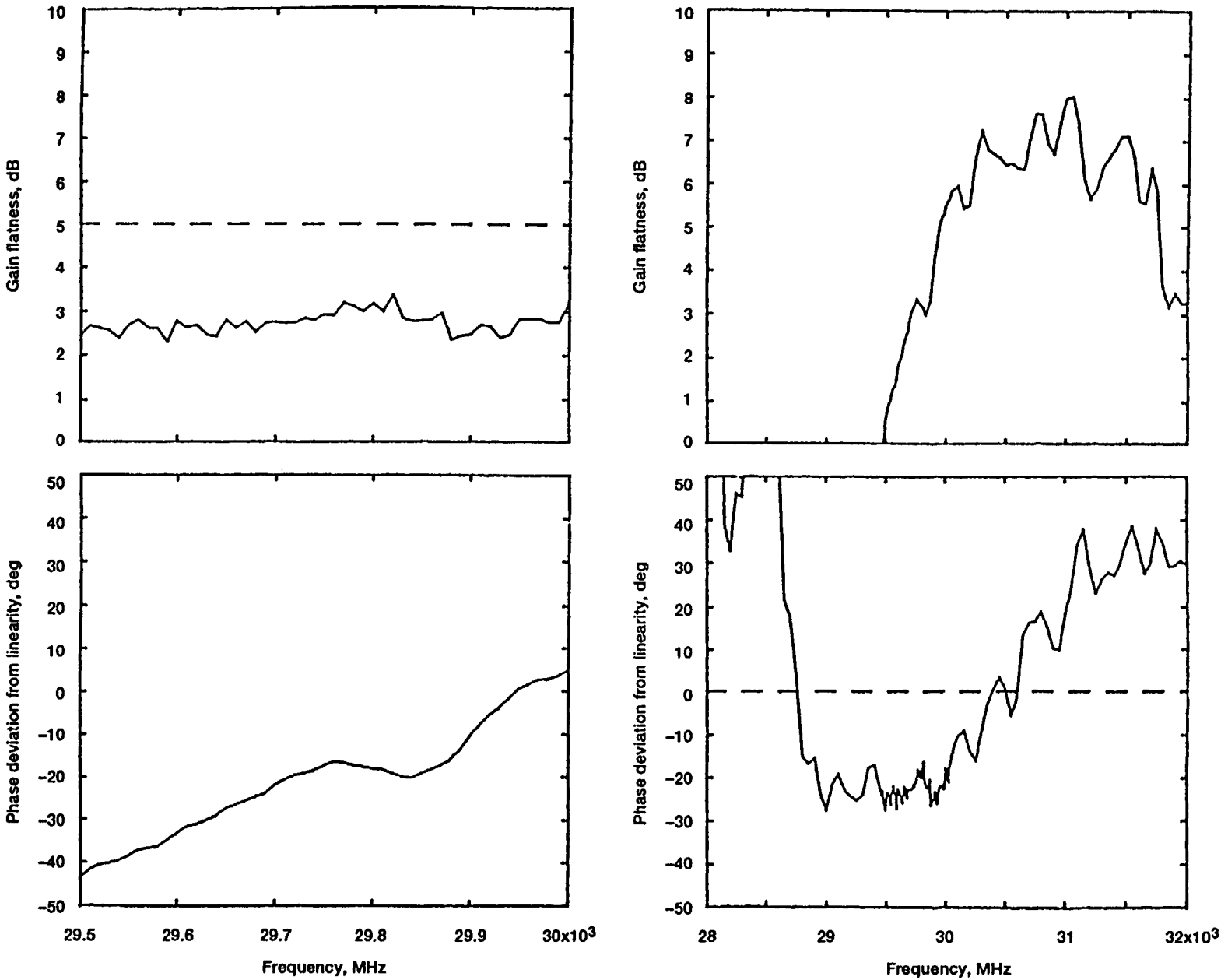

Figure 41.—Relationship of gain flatness to phase deviation from linearity for tube 2 at 16.0 kV and saturation –6 dB.

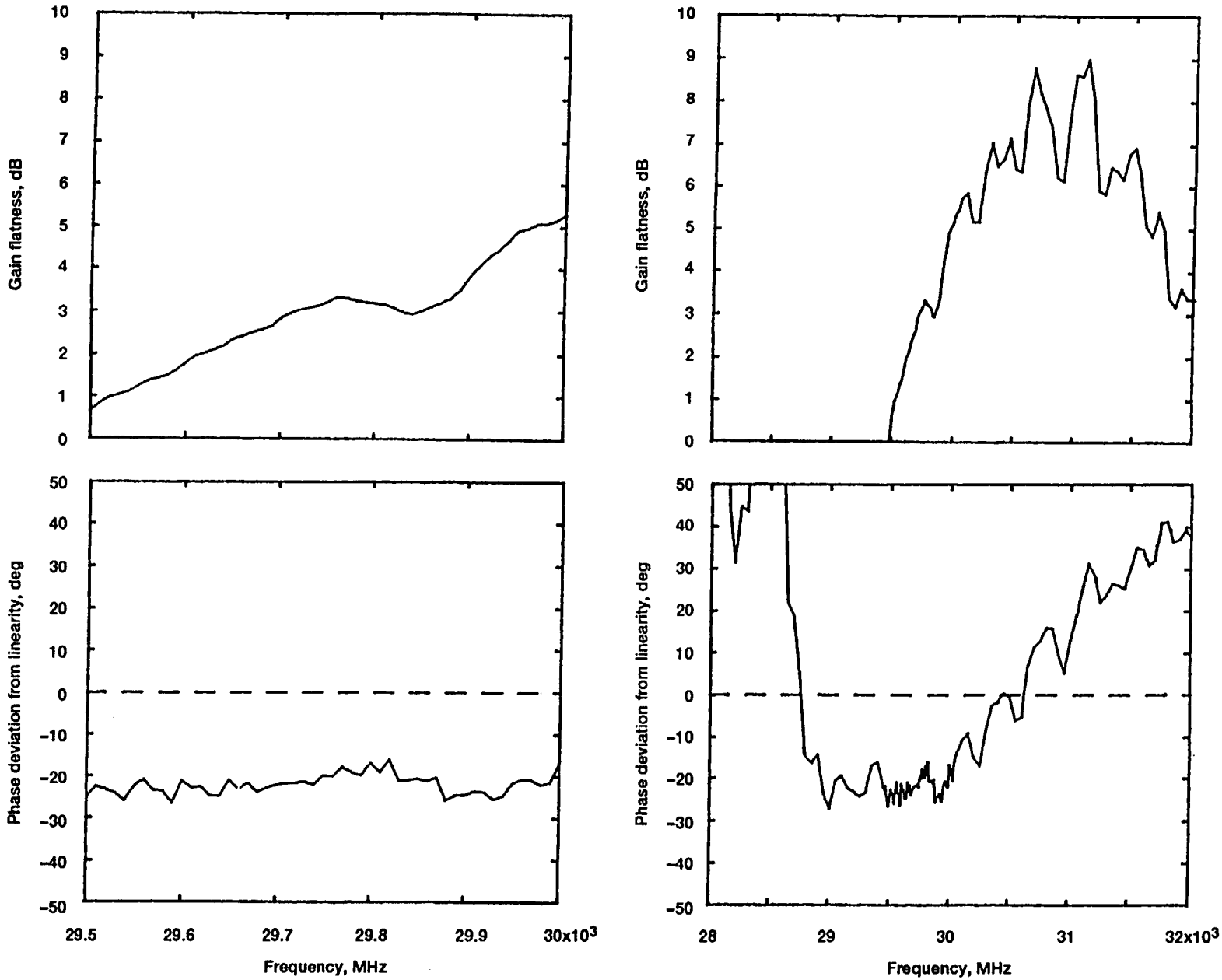

Figure 42.—Relationship of gain flatness to phase deviation from linearity for tube 2 at 16.0 kV and saturation -10 dB.

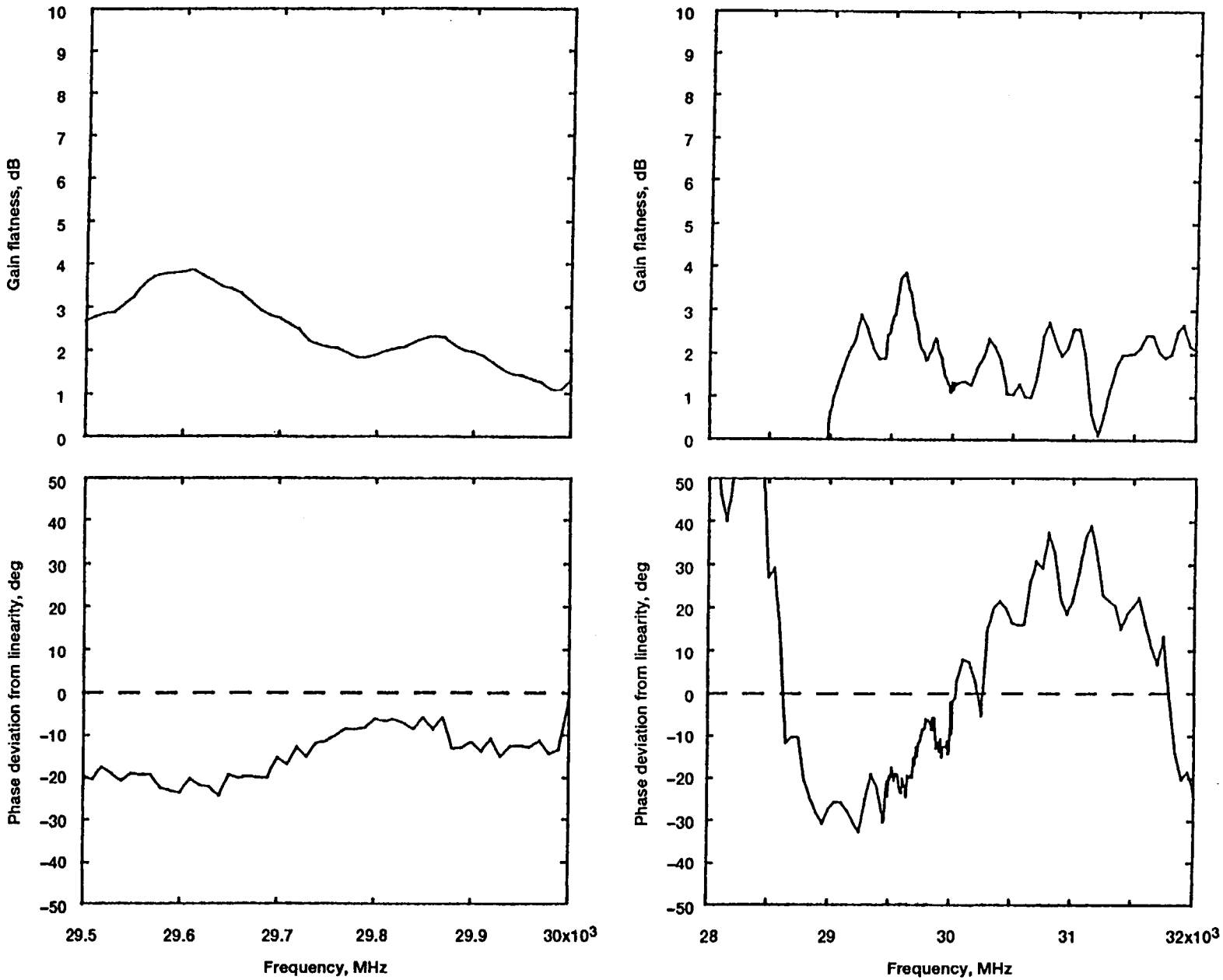

Figure 43.—Relationship of gain flatness to phase deviation from linearity for tube 2 at 16.25 kV and saturation.

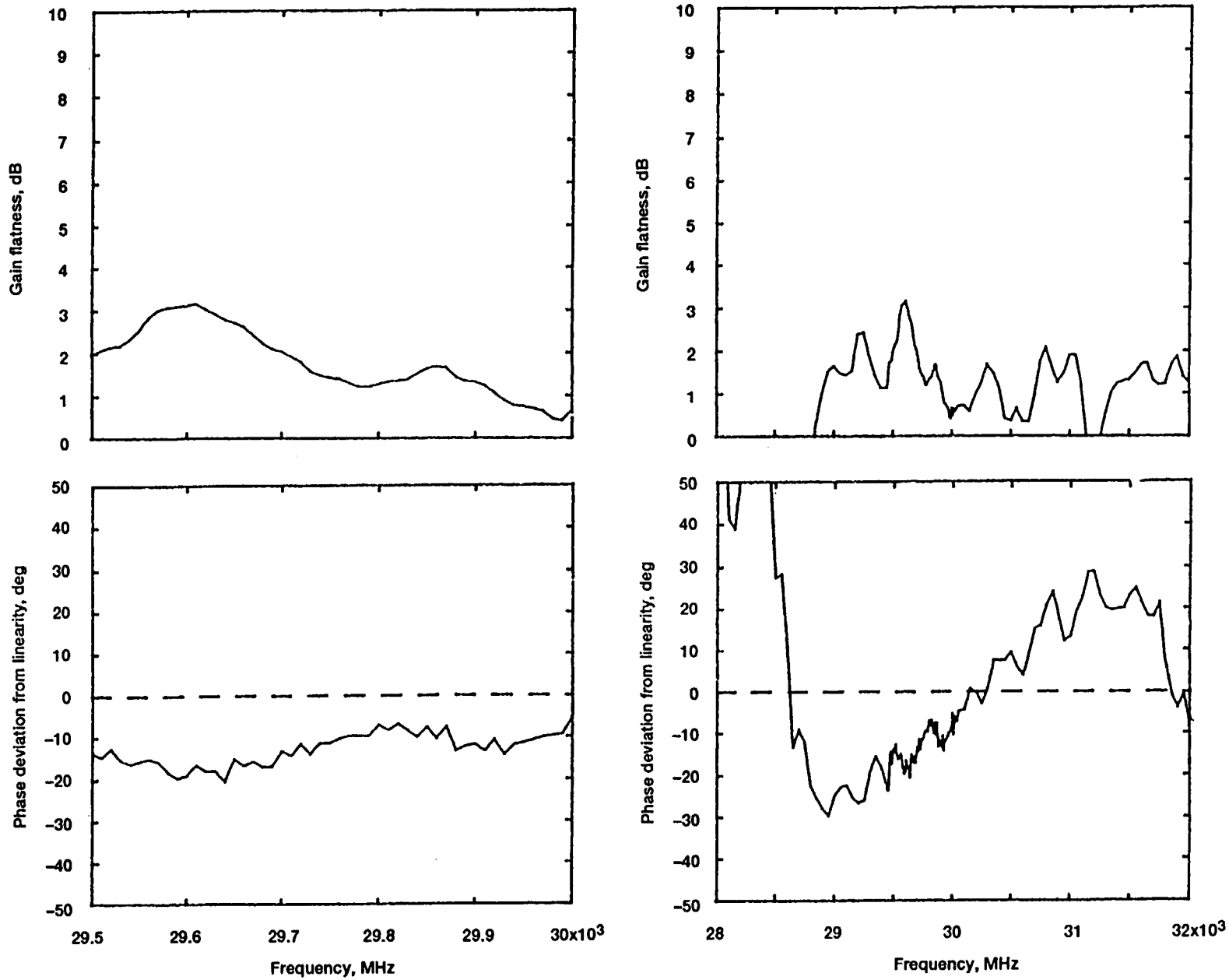

Figure 44.—Relationship of gain flatness to phase deviation from linearity for tube 2 at 16.25 kV and saturation +1 dB.

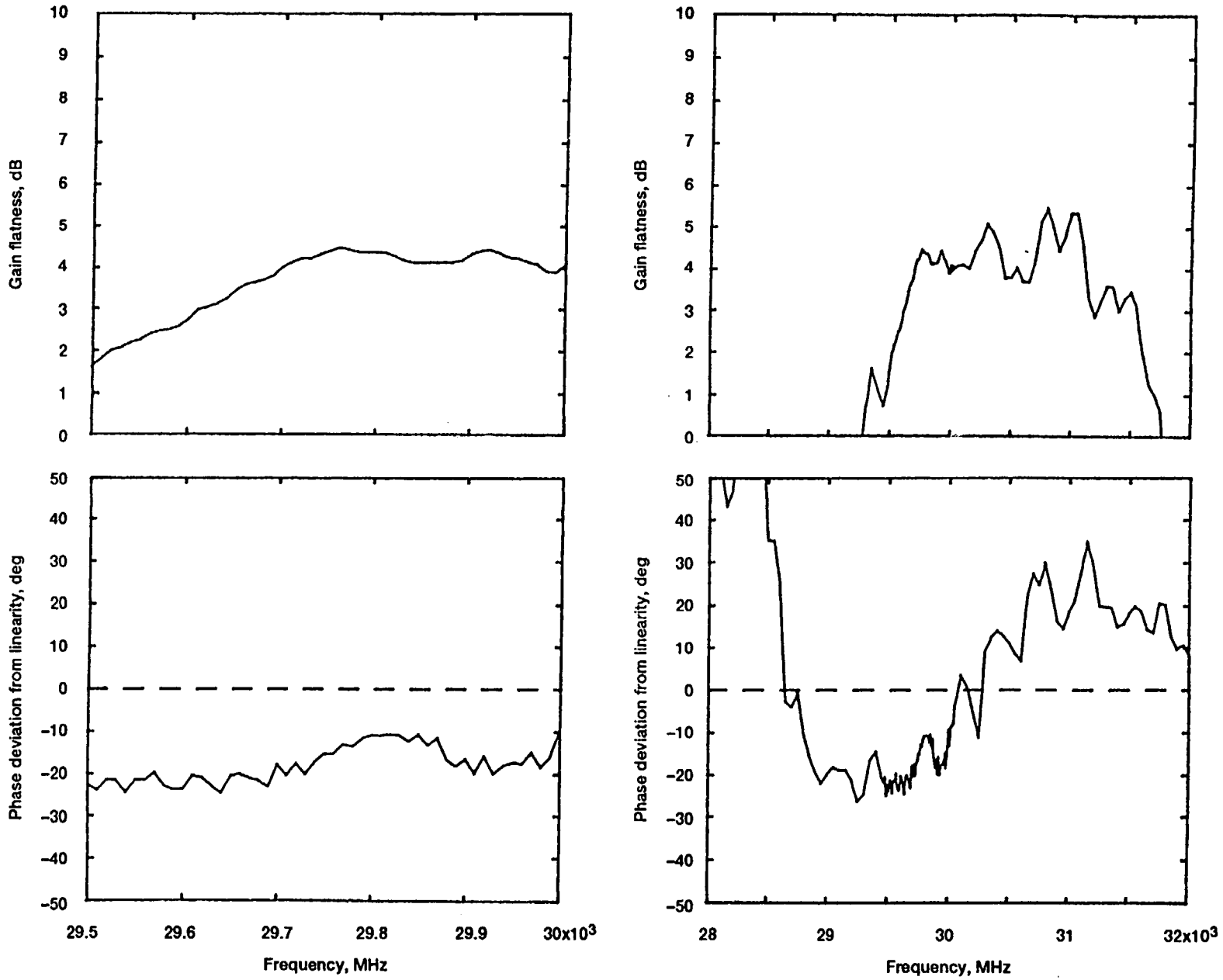

Figure 45.—Relationship of gain flatness to phase deviation from linearity for tube 2 at 16.25 kV and saturation -3 dB.

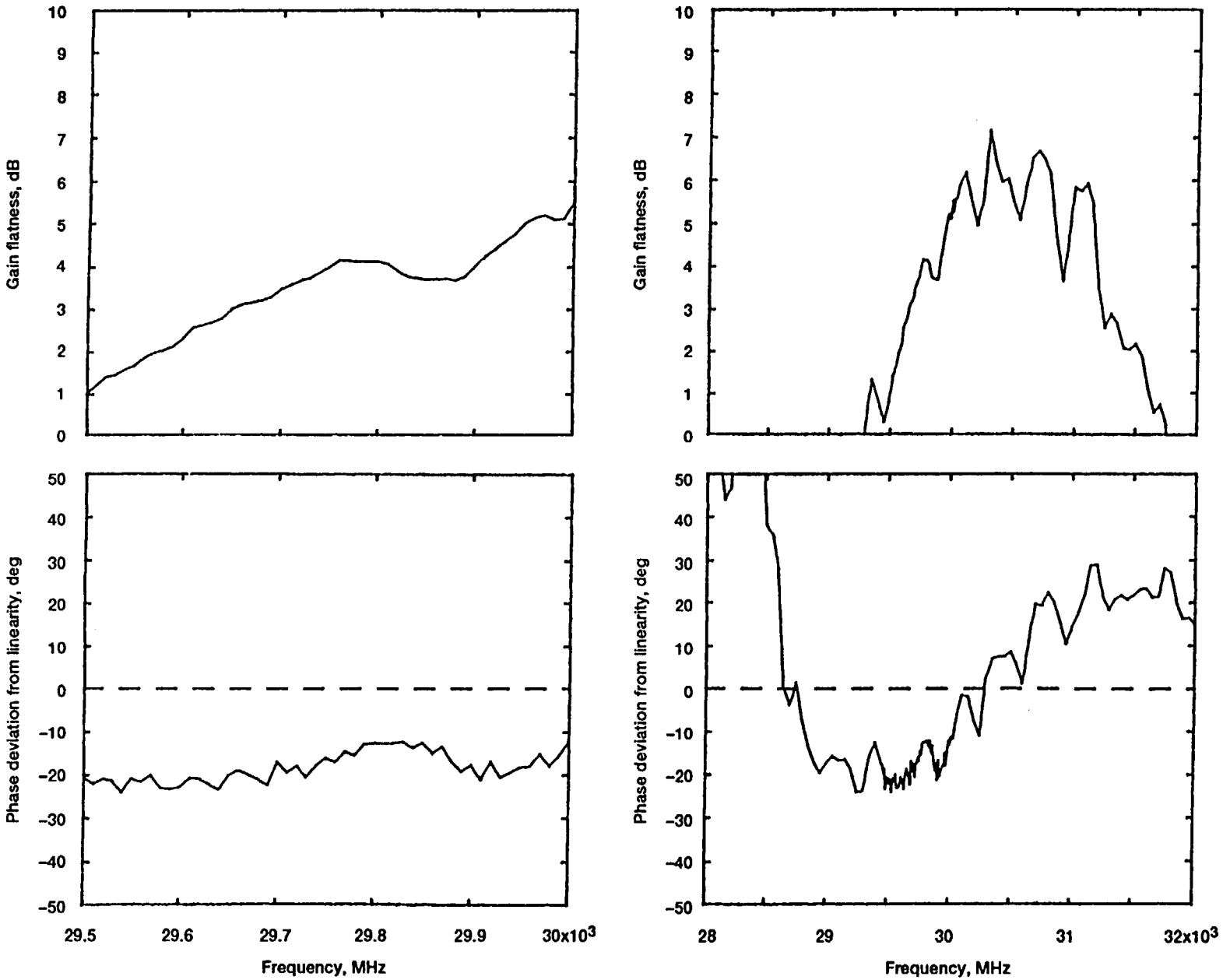

Figure 46.—Relationship of gain flatness to phase deviation from linearity for tube 2 at 16.25 kV and saturation –6 dB.

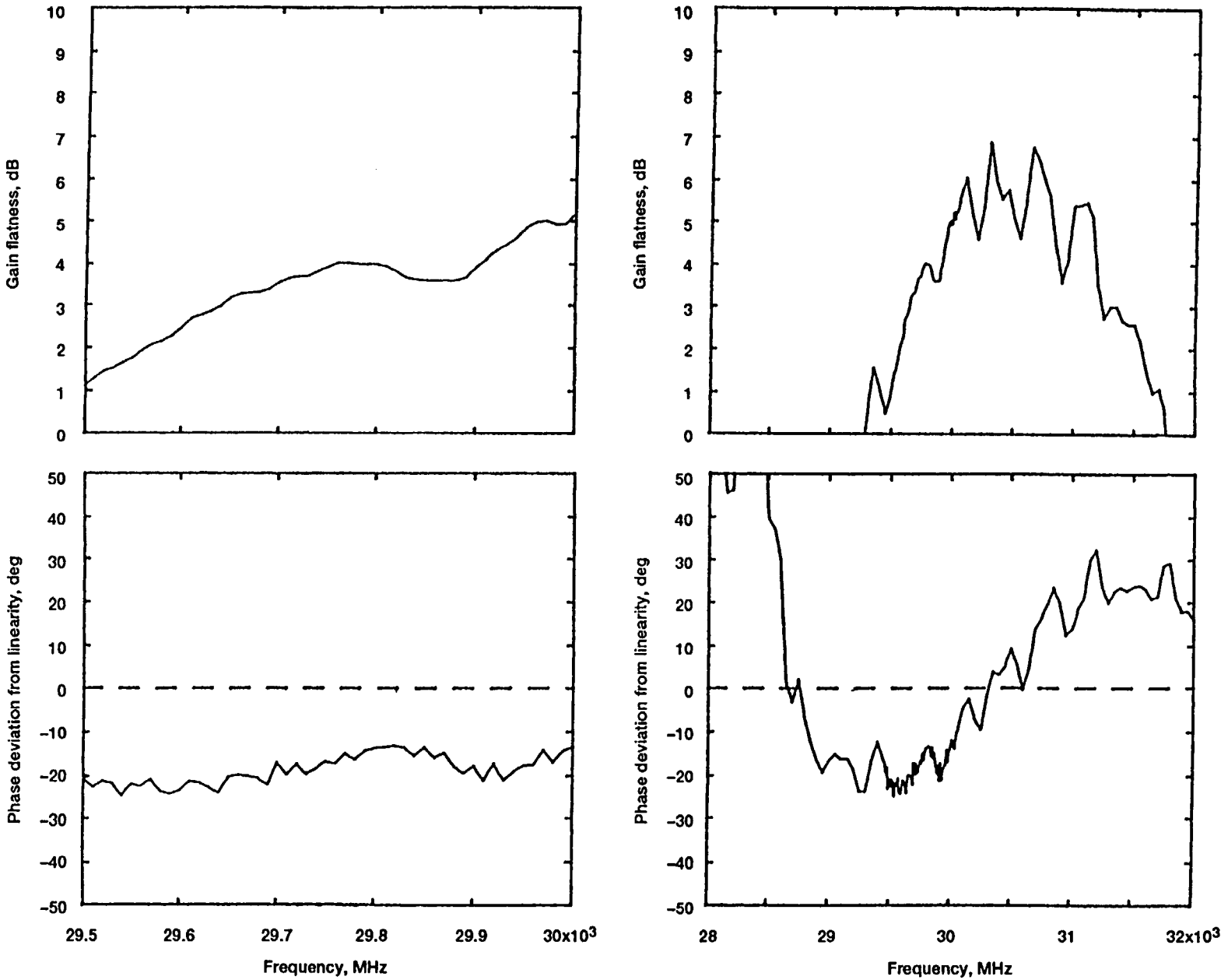

Figure 47.—Relationship of gain flatness to phase deviation from linearity for tube 2 at 16.25 kV and saturation -10 dB.

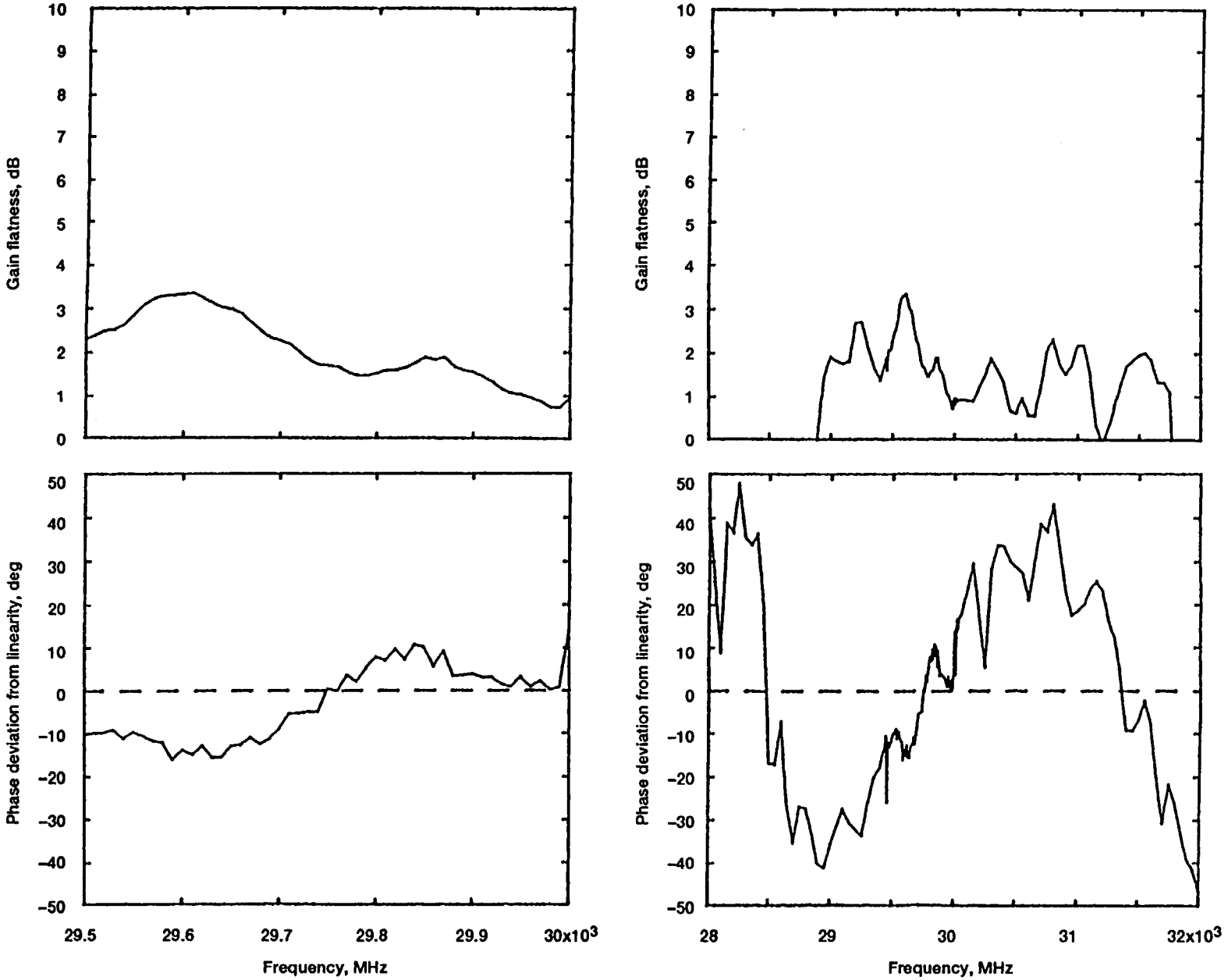

Figure 48.—Relationship of gain flatness to phase deviation from linearity for tube 2 at 16.5 kV and saturation.

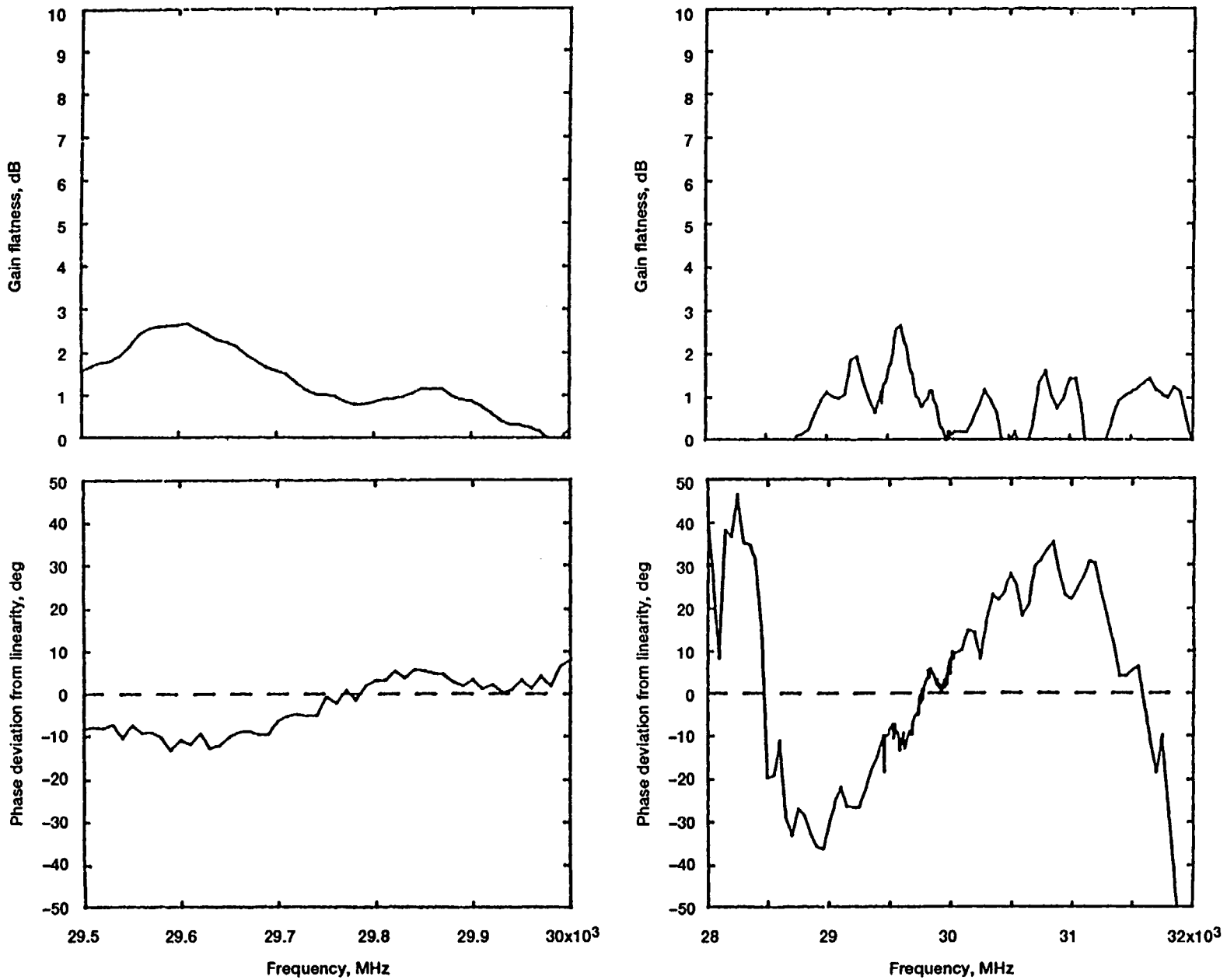

Figure 49.—Relationship of gain flatness to phase deviation from linearity for tube 2 at 16.5 kV and saturation +1 dB.

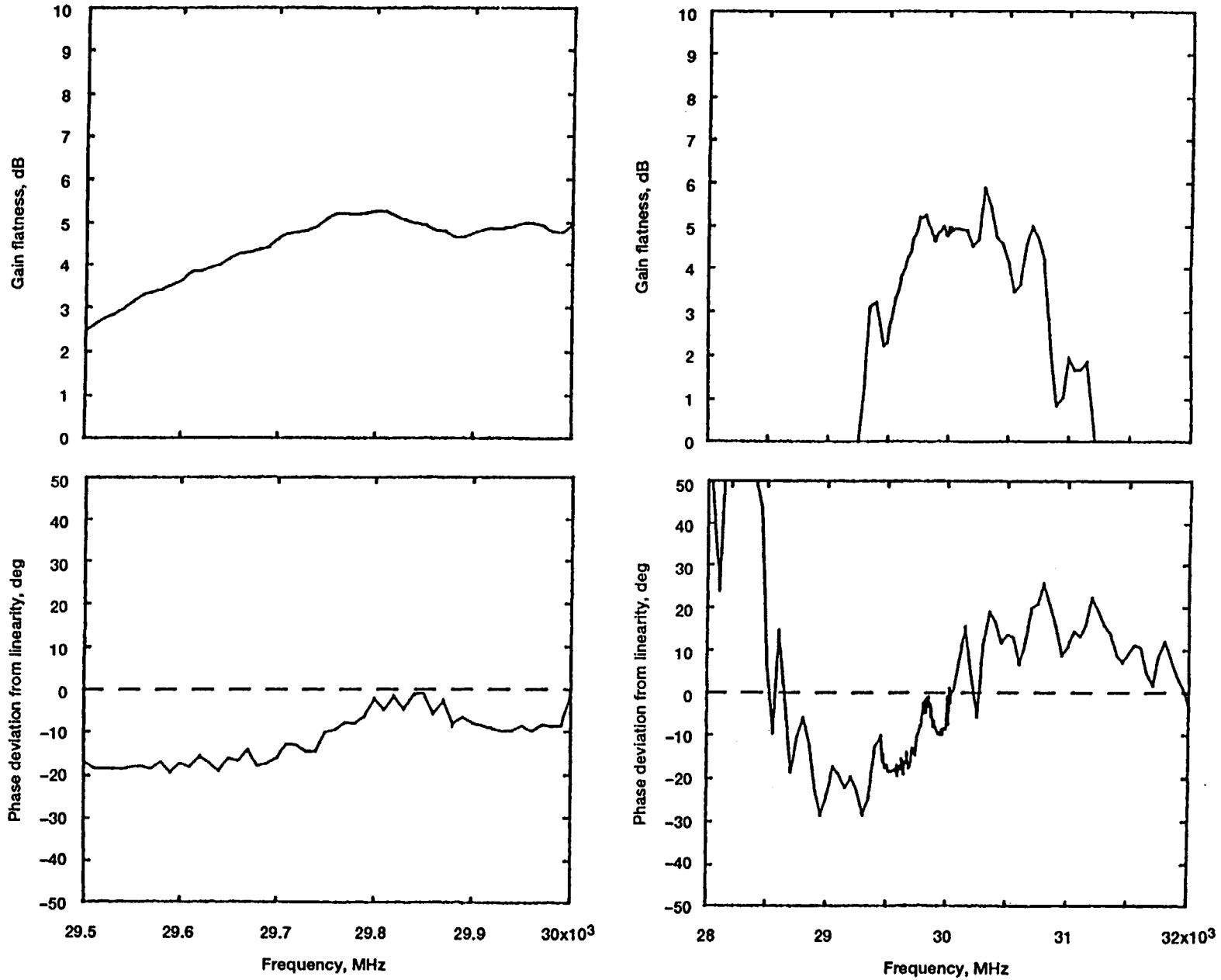

Figure 50.—Relationship of gain flatness to phase deviation from linearity for tube 2 at 16.5 kV and saturation –3 dB.

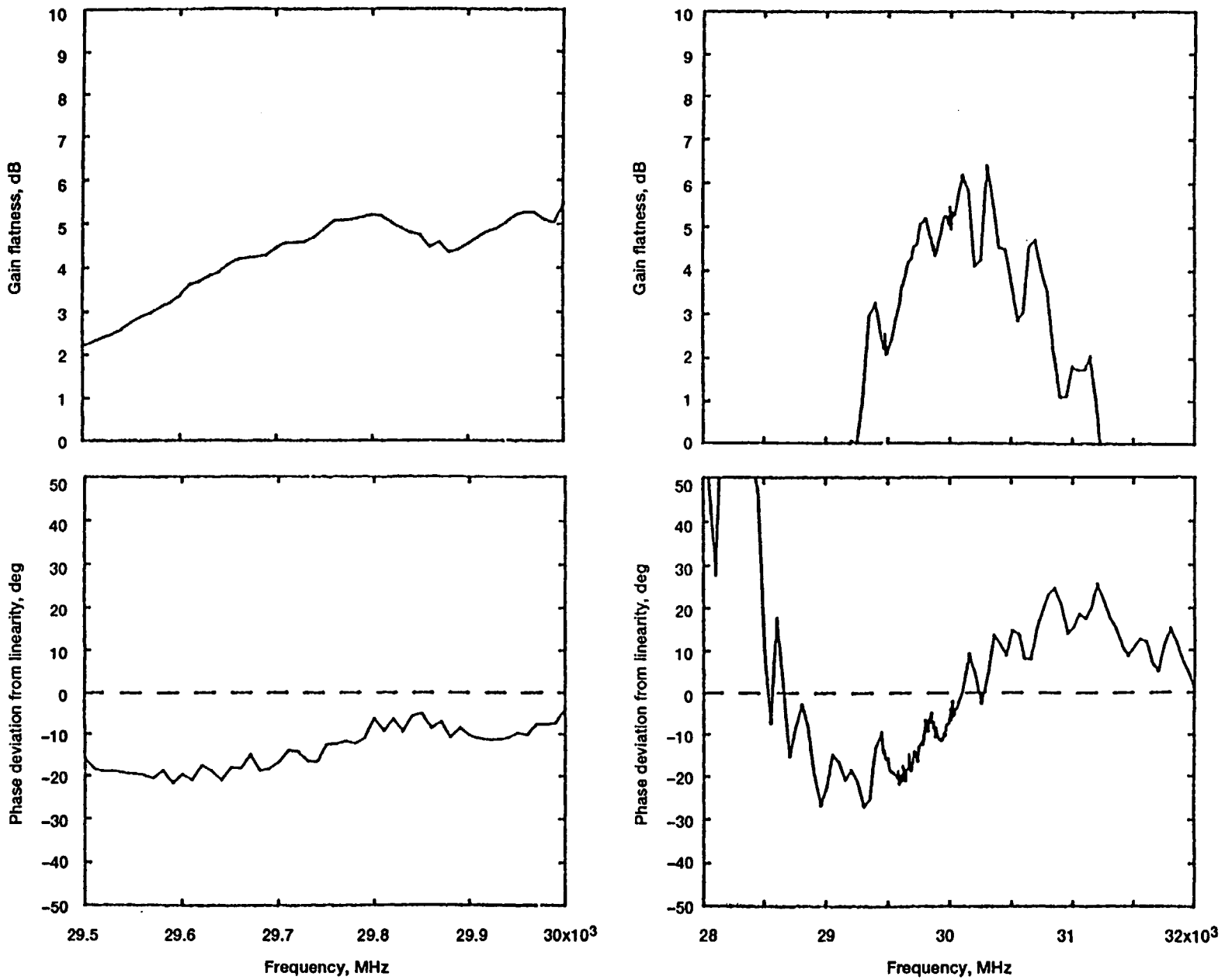

Figure 51.—Relationship of gain flatness to phase deviation from linearity for tube 2 at 16.5 kV and saturation -6 dB.

REFERENCES

1. Wallander, S.O.: Reflections and Gain Ripple in TWT's. IEEE Trans. Electron Devices, vol. ED-19, no. 5, May 1972, pp. 655-663.

2. Engineering Bulletin. Internal Document. Varian Assoc., Palo Alto, CA, Jan. 1966.

3. Beam, W.R.; and Blattner, D.J.: Phase Angle Distortion in Traveling-Wave Tubes. RCA Rev., vol. 17, Mar. 1956, pp. 86-99.

4. Chaffee, F.: Design Study, Final Report. Contract No:73-78-C-0428, Litton Industries, San Carlos, CA, Aug. 1978.

5. Ober, J.: The Large Signal Behavior of a Traveling Wave Tube With an Attenuating Central Helix Section. Philips Res. Rep., vol. 20, 1956, pp. 357-376.

6. Nishihara, H.; and Terada, M.: Effects of Attenuator on the Nonlinear Phase and Distortion of a TWT. IEEE Trans. Electron Devices, vol. ED-17, no. 8, 1970, pp. 638-640.

7. Shalkhauser, K.P.; and Fujikawa, G.: Bit-Error-Rate Testing of High-Power 30 GHz Traveling Wave Tubes for Ground-Terminal Applications. NASA TP-2635, 1986.

REPORT DOCUMENTATION PAGE

Form Approved
OMB No. 0704-0188

1. AGENCY USE ONLY (*Leave blank*)	2. REPORT DATE	3. REPORT TYPE AND DATES COVERED
	January 1994	Final Contractor Report

4. TITLE AND SUBTITLE

Phase Linearity of the 914H Coupled-Cavity Traveling Wave Tube

5. FUNDING NUMBERS

WU–506–72
C–NAS3–25776

6. AUTHOR(S)

Frank E. Kavanagh

7. PERFORMING ORGANIZATION NAME(S) AND ADDRESS(ES)

Analex Corporation
3001 Aerospace Parkway
Brook Park, Ohio 44142

8. PERFORMING ORGANIZATION REPORT NUMBER

E–7830

9. SPONSORING/MONITORING AGENCY NAME(S) AND ADDRESS(ES)

National Aeronautics and Space Administration
Lewis Research Center
Cleveland, Ohio 44135–3191

10. SPONSORING/MONITORING AGENCY REPORT NUMBER

NASA CR–191056

11. SUPPLEMENTARY NOTES

Project Manager, James A. Dayton, Space Electronics Division, (216) 433–3515.

12a. DISTRIBUTION/AVAILABILITY STATEMENT

Unclassified - Unlimited
Subject Category 32

12b. DISTRIBUTION CODE

13. ABSTRACT ***(Maximum 200 words)***

Tests of phase deviation from linearity were made on two 914H coupled-cavity traveling wave tubes (TWT). One tube had a voltage standing wave ratio (VSWR) of 2.4 and the other 1.4. The data showed that phase deviation is primarily a function of the amplitude and shape of the output VSWR. It was predicted that the low-VSWR tube would give better system performance than the tube with a high VSWR. This prediction was confirmed by the Advanced Communications Technology Satellite (ACTS) system tests performed at the NASA Lewis Research Center. A possible improvement in the construction and stability of coupled-cavity TWT's is discussed.

14. SUBJECT TERMS	15. NUMBER OF PAGES
Coupled-cavity; Traveling wave tube; Phase linearity; Satellite communications	52
	16. PRICE CODE: A03

17. SECURITY CLASSIFICATION OF REPORT	18. SECURITY CLASSIFICATION OF THIS PAGE	19. SECURITY CLASSIFICATION OF ABSTRACT	20. LIMITATION OF ABSTRACT
Unclassified	Unclassified	Unclassified	